7-2015

Characterization of the Effects of bFGF and GSK3β Inhibitors on Embryoid Bodies Derived from Human Pluripotent Stem Cells

Jonathan Earls
University of Arkansas, Fayetteville

Characterization of the Effects of bFGF and GSK3β Inhibitors on Embryoid Bodies Derived from Human Pluripotent Stem Cells

A thesis submitted in partial fulfillment
of the requirements for the degree of
Master of Science in Biomedical Engineering

by

Jonathan Earls
University of Arkansas
Bachelor of Science in Physics, 1998

July 2015
University of Arkansas

This thesis is approved for recommendation to the Graduate council.

_____

Dr. Kaiming Ye
Thesis Director

_____

Dr. Sha Jin
Thesis Co-director:

_____

Dr. Robert Beitle
Thesis Committee

ABSTRACT

Embryoid body (EB) formation is a common first step in many human pluripotent stem cell (hPSC) differentiation protocols. Previous work suggests that EBs are sensitive to growth factor withdrawal if they are derived from hPSCs maintained in feeder independent media such as mTeSR1. To promote cell survival, EBs generated from mTeSR1-adapted hPSCs are sometimes cultured in a medium that contains basic fibroblast growth factor (bFGF), a trophic factor often used in hPSC cultures to maintain self-renewal. This distinguishes feeder independent hPSCs from feeder dependent hPSCs. The purpose of this study was to characterize the effects of bFGF as well as small molecule inhibitors of GSK3β on the formation, growth, cell-cell signaling and early fate decisions of human EBs. bFGF or GSK3β inhibitor treated EBs grew in size and showed evidence of cell proliferation. Control EBs that were fed only a basal serum free EB medium without added growth factors tended to fall apart in culture, adopted irregular morphologies and showed no signs of growth or proliferation. Changes in cell-cell adhesion commonly observed in differentiating hPSCs were apparent in the bFGF and BIO treated EBs, while untreated control EBs predominantly expressed E-cadherin, a cell-cell adhesion molecule highly expressed in undifferentiated hPSCs. Expression of pluripotency markers decreased in all EB groups, regardless of treatment, and increased germ layer marker expression was detected in all groups, with a particular bias towards neuroectoderm. Our results suggest a role for GSK3β in the development and survival of EBs derived from feeder independent hPSCs. These results could inform the development of protocols for the directed differentiation of feeder independent hPSCs using defined media and small molecules.

Acknowledgement

I would like to thank my Coadvisors, Drs. Kaiming Ye and Sha Jin for giving me the opportunity to pursue stem cell research. I would also like to thank Dr. Robert Beitle for being a part of my advising committee. I would like to thank my labmates Weiwei Wang, Han Lei, and Qing Long for helping me to optimize my immunostaining and western blot protocols. Thanks to Yu Wen for loaning me some of her IMR90's. Special thanks as well to my other lab mates Lu, Yarina, Andreas, Ngoc, Huantong Yao and Hanan for being good people.

Of course I'd like to thank my family for their love and support.

Table of Contents

List of Figures

Chapter 1 – LITERATURE REVIEW

1.1 Introduction

Human pluripotent stem cells (hPSCs), including human embryonic stem cells (hESCs) and human induced pluripotent stem cells (hiPSCs), can proliferate indefinitely in culture and can in principle differentiate into any of the more than 200 cell types in the human body[1-3]. These properties, known respectively as self-renewal and pluripotency, make hPSCs attractive as potential cell sources for applications in drug discovery, toxicology, disease modeling and eventually regenerative medicine, and as such hPSCs have become the subject of intense research focus.

hESCs were first isolated from the inner cell mass of 5-6 day old human blastocysts in 1998. Since the immunosurgery technique used to derive a hESC line renders the embryo nonviable, there is a tremendous ethical controversy surrounding the use of hESCs for research or in the clinic. As a result of these ethical concerns, federal funding for hESC research in the United States has been limited to just a few approved hESC lines.

In 2007, hiPSCs were generated from human fibroblasts by retroviral induction of just four transcription factors: Oct4, Sox2, Klf4 and C-myc. Since then numerous methods for the induction of pluripotency in human somatic cell types have been developed, including retroviral, lentiviral or adenoviral induction of different combinations of transcription factors, non-integrating episomal vectors, transposon vectors, and delivery of synthetic RNA molecules [4-9]. hiPSCs are phenotypically and functionally similar to hESCs, and they are promising cell lines for both research and clinical applications[10]. Patient specific hiPSCs may be generated and subsequently used for disease modeling or cell therapies, and these hiPSC derived cells might carry less risk for immune rejection than an equivalent hESC derived transplant, though this point is controversial [11].

Examples of cell therapies utilizing hPSC derived cells include dopaminergic neurons to treat Parkinson's disease, glial precursors to treat spinal cord injury, pancreatic β-cells to treat type I diabetes, and cardiomyocytes to treat congestive heart failure to name just a few [12-15]. The strategies devised for the implementation of these therapies are similar in that they each involve the replacement of a single cell

type that has lost function. Current methods for generating these replacement cell types are similar as well. hPSCs are expanded and then induced to differentiate into the desired cell type (e.g. dopaminergic neuron or progenitor cell) *in vitro*, often employing growth factors or small molecules that activate signaling pathways known to be involved in early embryological development. The target cell types are purified, and in some cases they are expanded and allowed to mature before transplantation into the patient. To date, only three Phase I/II clinical trials involving hPSC derived cells have been conducted or begun in the U.S.A. One of these trials—to treat spinal cord injuries with glial precursors derived from hESCs-- was halted early due to financial concerns, not concerns about safety or efficacy [16]. The other two trials—to treat age related macular degeneration and Stargardt's Macular Dystrophy with hESC derived retinal pigment epithelial cells—are ongoing and have reported some early success [17]. However, despite rapid progress, most hPSC research is still focused on *in vitro* studies and non-human animal models, and the long term safety and efficacy of hPSC derived cell therapies is not yet established [15].

hPSCs might find more immediate use in drug discovery [18, 19]. Many drug candidates that are effective in murine models of disease are not effective in humans, so it would be advantageous to develop reliable human preclinical models to assess the efficacy and toxicity of candidate drug molecules before too many resources are committed to their development. hPSCs offer a virtually unlimited supply of differentiated cell types that are important for drug metabolism or are particularly vulnerable to the effects of drug toxicity, such hepatic or cardiac cells. hPSCs also provide a useful model for early human development as well as human disease progression [19]. Numerous hiPSC lines have been generated to model diseases such as Down syndrome, Fanconi anemia, Huntington's disease and schizophrenia [20-23].

1.2 Maintenance of hPSC Self-Renewal

hPSCs are characterized by high expression of transcription factors such as Oct4, Nanog, and Sox2 as well as membrane antigens SSEA3, SSEA4, Tra-160 and Tra-181 [24,25]. Oct4, Nanog, and Sox2 form a regulatory network that maintain self-renewal and pluripotency by co-occupying the promoter regions of hundreds genes associated with repressing differentiation [26]. They are alkaline phosphatase positive, grow in compact colonies and have a high nuclear to cytoplasmic ratio.

The pathways that contribute to hPSC self-renewal differ somewhat from those involved in murine PSC (mPSC) self-renewal. For instance, treatment with LIF and BMP4 are known to promote mPSC self-renewal, while LIF has no effect on hPSC self-renewal and BMP4 actively promotes hPSC differentiation [24]. Numerous groups have found that hPSC self-renewal depends on basic fibroblast growth factor (bFGF) as well as Activin A, TGFβ1 and IGF-1 [27-29]. These signaling proteins activate intracellular pathways such as Raf/ERK, PI3K/AKT and SMAD2/3, which in turn regulate the transcriptional circuitry that maintains self-renewal and pluripotency [30]. Curiously, the requirement of bFGF and Activin A in hPSC maintenance culture makes hPSCs more similar to post implantation mouse epiblast stem cells than mPSCs [31].

Three general methods have been developed for the maintenance and expansion of hPSC populations *in vitro*: feeder dependent, feeder free, and feeder independent. The feeder dependent method is the oldest and is still commonly used. hPSC colonies are cocultured with mitotically inactivated mouse embryonic fibroblasts (MEFs) or in some cases human fibroblast feeders [1, 32]. Typically the coculture is fed a base medium consisting of DMEM or DMEM/F12 and a commercially available serum replacement to which a small amount of bFGF is added. bFGF acts on the hPSCs themselves by activating Erk signaling and the PI3K/Akt pathway, as well as stimulating the MEFs to secrete growth factors which then stimulate the hPSCs.

These secreted factors include transforming growth factor β1 (TGFβ1), Activin A, various heparan sulfate proteoglycans, and gremlin (an inhibitor of BMP signaling)[33, 34]. In 2001, Xu *et al*. demonstrated that culturing hESCs in a bFGF containing medium that had been conditioned by MEFs was sufficient to maintain self-renewal [35]. The hESCs were cultured in dishes coated in Matrigel, an extracellular matrix extract derived from the murine Engelbreth-Swarm tumor that is rich in laminin and collagen IV [36]. This culture method is sometimes called feeder-free culture.

Though effective and widely used, the feeder dependent and feeder-free culture methods have significant drawbacks [37]. The feeder dependent method is time and labor intensive, making scale-up of hPSC cultures difficult. And both the feeder dependent and feeder-free systems rely on factors secreted by cells of non-human origin (MEFs), complicating the process of FDA approval of cell therapies derived

from hPSCs. For example, hESC derived retinal pigment epithelial cells currently being explored as a treatment for Stargardt's Macular Dystrophy are classified as a xenotransplant, since the hESCs were originally cocultured with MEFs [17]. The undefined nature of feeder based culture systems also makes it difficult to standardize hPSC protocols and replicate experimental results obtained in different laboratories [37].

Feeder dependent methods for maintaining hPSCs have led to contamination of those hPSC lines with non-human molecules. MEF dependent hESCs as well as embryoid bodies (EBs) derived from those hESCs metabolically incorporate a non-human sialic acid, Neu5Gc [38]. Many people have antibodies against Neu5Gc circulating in their blood, and so there is a risk that feeder dependent hPSC-derivatives could elicit an immune response upon transplantation into a patient. This could limit the clinical use of hPSC derived cells.

These difficulties have motivated the development of hPSC culture mediums that do not rely on MEF coculture or MEF conditioned medium at all. So-called feeder independent media are supplemented with growth factors and small molecules found to support hPSC self-renewal in analyses of MEF conditioned media. Several feeder independent hPSC maintenance media have been developed, some of which are commercially available.

One of the most popular feeder independent media is mTeSR1 [39]. Compared to MEF conditioned media, mTeSR1 has a very high concentration of bFGF (100 ng/ml). This high concentration bFGF was found to suppress BMP signaling [40]. mTeSR1 also contains TGFβ1, lithium chloride (LiCl), GABA and pipecolic acid [39]. LiCl is a small molecule inhibitor of glycogen synthase kinase 3β (GSK3β), and it is included in mTeSR1 based on a report by Sato *et al*. indicating that activation of canonical *Wnt* signaling *via* the chemical inhibition of GSK3β enhances hESC self-renewal [41]. GABA and its cofactor pipecolic acid are included in mTeSR1 based on the observation that undifferentiated hESCs express the GABA receptor [42]. Excluding any one of the 5 pluripotency factors results in a loss of proliferative capacity or down regulation of one or several markers of pluripotency [28].

mTeSR1 is not free of animal products, nor is the mTeSR1 culture system completely defined. mTeSR1 contains bovine serum albumin, and it is common for mTeSR1 adapted hPSCs to be cultured on plates coated with Matrigel. A xeno-free version of mTeSR1, TeSR2 is also available, and some groups have replaced the Matrigel substrate with human vitronectin, laminin 511 or synthetic peptides that mimic the binding sites of various extracellular matrix molecules, thereby making it possible to maintain and expand hPSCs in a completely xeno-free environment [43-45]. Recently a simplified form of xeno-free TeSR, called E8, has become commercially available. Unlike TeSR2, E8 does not contain human albumin, and this omission promises to significantly reduce the costs associated with the use of defined xeno-free media [46].

1.3 Similarities and differences between Feeder dependent and feeder independent cultures

In 2010, the International Stem Cell Consortium compared eight feeder independent media and found that only two, Stempro and mTeSR1, were able to support the undifferentiated growth of hESCs for 10 passages[47]. According to Yoon *et al*., hESCs maintained in mTeSR1 have a global gene expression profile that is similar to feeder dependent hESCs[48]. They readily form teratomas, a standard test of pluripotency, and some groups report that the directed differentiation efficiencies of mTeSR1 adapted hPSCs are comparable to feeder dependent/free hPSCs [28, 49].

Nevertheless, there is accumulating evidence that hPSCs maintained in feeder independent mediums such as mTeSR1 are not identical to their feeder dependent counterparts. MEF dependent and mTeSR1 adapted hESCs have differing FTIR spectra, suggesting differing macromolecular compositions [50]. Specifically mTeSR1 adapted hPSCs have greater amounts of phosphorylated molecules and higher amino acid concentrations, while MEF dependent hPSCs have higher levels of carbohydrates. These differing compositions remain even after the hPSCs are induced to differentiate into mesoderm. The authors speculated that differences in endogenous production of growth factors or epigenetic changes in the hPSCs may account for their observations.

Tompkins *et al.* found that mTeSR1 adapted hPSCs accumulate numerous transcriptional and epigenetic changes that do not go away upon conversion to feeder dependent culture[51]. Blauwkamp *et al.* reported that hESCs cultured in mTeSR1 rapidly differentiate in response to exogenous *Wnt*3a, while

canonical *Wnt* signaling promotes the expansion of undifferentiated MEF dependent hESCs [52]. The authors linked this difference in the effects of growth factor stimulation to the presence of lysophosphatidic acid (LPA) in the knock out serum replacement fed to the MEF dependent hESCs. LPA is not a component of mTeSR1. However, when LPA was added to mTeSR1, the feeder independent hPSCs responded to *Wnt* signaling in much the same way as MEF dependent cultures, thus demonstrating the influence of medium composition on hPSCs' response to exogenous growth factors.

Another group has reported that hPSC maintenance culture conditions affect the efficiency of differentiation to cardiac lineages [53]. mTeSR1 adapted hESCs yielded significantly fewer cardiomyocytes than feeder dependent cultures. The authors also noted that mTeSR1 adapted hESCs expressed the neuroectoderm marker NCAM1 even when undifferentiated, suggesting that prolonged culture in mTeSR1 might partially neuralize hPSCs.

1.4 Embryoid Bodies

Differences between feeder dependent and mTeSR1 adapted hPSCs are also apparent in some of the protocols developed for the formation of embryoid bodies (EBs). EBs are multicellular aggregates that spontaneously form when hPSC colonies are removed from adherent conditions and cultured in suspension. Cells within the EBs differentiate into cell types from all three germ layers, and so, along with teratoma formation, the ability to form EBs constitutes a functional test of pluripotency.

To a certain extent, EBs recapitulate the development of early embryos[54]. Unlike EBs generated from embryonic carcinomas, EBs derived from mPSCs and hPSCs display a remarkable degree of self-organization[55, 56]. As mPSCs within the aggregates begin to differentiate, pluripotency markers such as *Oct4* and *Nanog* are transcriptionally down-regulated. Cells near the outside surface of the EB give rise to primitive endoderm, which further differentiates into visceral and parietal endoderm [57]. This extraembryonic endoderm secretes a basement membrane rich in laminin and collagen IV that separates the outer endoderm layer from an inner pluripotent epiblast layer (**Fig. 1.1**) [56, 58]. After a few days in culture, EBs develop a shell of collagen I, reducing nutrient diffusion into the EBs' interior[59]. In extended culture, cells in the center of EBs tend to commit apoptosis, and the EBs become hollow in a process called cavitation. It is believed that cavitation occurs as a result of epiblast cells losing contact with the

basement membrane as well as decreased nutrient and oxygen diffusion into the EBs' interior as they grow in size [60,61]. Decreased soluble factor diffusion to the center of an EB also creates an interior signaling gradient, which allows for the emergence of numerous cell types within a single EB. The heterogenous nature of EB culture can present difficulties for hPSC directed differentiation protocols, where generating a pure population of differentiated cell types at high efficiency is desired.

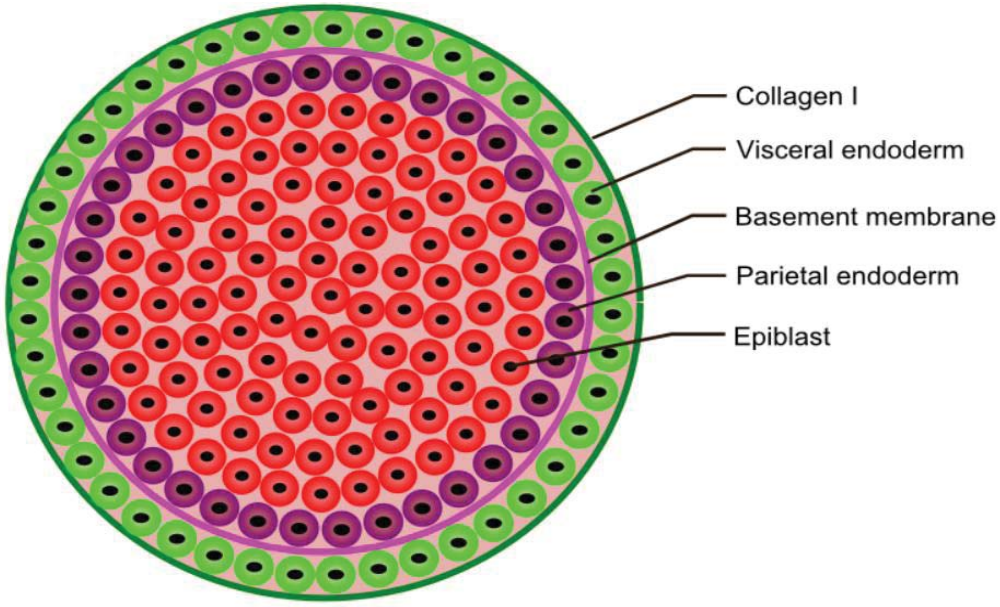

Figure 1.1. Cross-section of an embryoid body (EB).

Nonetheless EB formation is a common first step in many protocols for directing the differentiation of hPSCs. The EB model provides a biomimetic, three-dimensional environment that allows for complex cell-cell interactions that are difficult to achieve in monolayer cultures, and unlike many monolayer differentiation protocols, EB culture is compatible with some of the scale-up strategies that have already been developed for hPSC differentiation, such as stirred tank bioreactors and orbital shakers [62].

EBs are often fed with growth factors and small molecules in order to drive their specification towards a particular cell lineage. Methods of producing EBs in the presence of polymers which release soluble factors from within the EBs in a time controlled manner have been developed in order to reduce signaling gradients within EBs and promote more homogenous differentiation [63]. Also it has been observed that the size of an EB influences the lineage choices of the cells within the EBs. Methods for

producing size controlled human EBs from single cell suspensions using forced aggregation in non-adherent 96 well plates or microwells have recently been developed, promising to increase the efficiency of EB based protocols [56, 64].

EB formation is often an intermediary step in an hPSC differentiation protocol, and the length of time the EBs are kept in suspension varies depending on the desired cell type. Cardiomyocyte and neural progenitor differentiation protocols often begin with an initial period of EB suspension culture followed by 2D monolayer culture, while many protocols for the generation of hematopoietic progenitors call for at least two weeks in suspension [65, 66]. EBs may be grown in suspension for many weeks if desired [67].

Traditionally when starting from feeder dependent hPSCs, bFGF is withdrawn from the culture medium upon EB formation [68]. In mTeSR1 adapted cultures, on the other hand, growing EBs in a serum-free medium without bFGF has been more difficult. This difficulty has motivated some research groups to abandon the EB method in favor of monolayer based differentiation protocols [69]. Antonchuk *et al* have previously reported that bFGF treatment of spin EBs generated from mTeSR1 adapted hPSCs greatly improves EB survival (personal correspondence) [70, 71]. Similar observations have been reported in mTeSR1 adapted EBs generated from cell clumps rather than single cells (personal correspondence) [72].

1.5 FGF signaling in early hPSC differentiation

bFGF is a trophic factor known to promote survival and proliferation in numerous cell types [73]. In adherent undifferentiated hPSCs, it prevents anoikis, a form of apoptosis resulting from loss of cell contact with the extracellular matrix [74]. According to Antonchuk *et al*., treating EBs with bFGF still allows for the emergence of cells from all three germ layers [71]. Even so bFGF plays a significant role in the lineage transitions of hPSCs and perhaps should not be regarded as neutral in terms of lineage commitment. bFGF is often used to induce neural differentiation in hPSCs [75-77]. Moreover the timing of FGF signaling during the early stages of differentiation can affect the efficiency of neural specification. Inhibiting bFGF/Erk during early hESC differentiation produces a larger population of cells expressing the neural stem cell marker Pax6 than non inhibited controls [78]. This suggests that early bFGF treatment

might attenuate neural differentiation. However after the $Pax6^+$ population emerges, bFGF treatment can increase CNS neural specification while decreasing PNS specification. Thus the effects of bFGF treatment on hPSC neural specification may depend on the differentiated state of the cells when they receive bFGF treatment.

bFGF can act as a competency factor in mesodermal differentiation. hESCs treated with BMP4 differentiate preferentially toward extraembryonic trophectoderm, but treating the hESCs with both BMP4 and bFGF switches the cells to a mesendodermal fate [79]. Through Mek/Erk signaling, bFGF prolongs Nanog expression, and it was found that enforced Nanog expression during BMP4 treatment could mimic the effect of bFGF treatment.

FGF sometimes influences cell fate by engaging in crosstalk with other signaling pathways. According to Israsena *et al*., bFGF treatment of neural stem cells (NSCs) induces nuclear localization of β-catenin and activation of canonical *Wnt* signaling, which then facilitates NSC proliferation and self renewal [80]. Crosstalk between FGF and canonical *Wnt* signaling plays a critical role during gastrulation [81]. mESCs with a mutant FGFR1 do not generate endoderm or cells that migrate through the primitive streak. These cells also fail to regulate E-cadherin. It was hypothesized that these high levels of E-cadherin sequestered β-catenin at adherens junctions, leaving it unavailable for participation in canonical *Wnt* signaling. Thus FGF signaling affects mesendodermal differentiation indirectly by modulating the available pool of β-catenin. In undifferentiated hPSCs, stimulation with bFGF is correlated with increased transient phosphorylation of AKT, Erk and GSK3β as well as activation of a *Wnt* luciferase reporter [82].

1.6 The Roles of Canonical *Wnt* Signaling and GSK3β in Regulating Self-Renewal and Early Differentiation of hPSCs

The canonical *Wnt* pathway is one of several signaling pathways thought to dominate early embryological development [83, 84]. In the absence of *Wnt* ligands, a destruction complex consisting of GSK3β, Axin, CK1 and APC cooperates to keep levels of cytoplasmic β-catenin very low. CK1 phosphorylates β-catenin at Ser45, which enables GSK3β to further phosphorylate β-catenin at Ser37 and Ser33 [85]. E3 ubiquitin ligase subunit βTrCP recognizes phosphorylated β-catenin, which is then quickly degraded [86]. When *Wnt* ligands bind to the transmembrane receptor Frizzled and its coreceptor

LRP 5/6, the intracellular protein Disheveled is activated, inducing the CK1 and GSK3β mediated phosphorylation of LRP 5/6. This creates a high affinity binding site for Axin at the cell membrane. Sequestering Axin at the membrane inhibits the formation of the destruction complex, and so the phosphorylation and degradation of β-catenin does not occur. Stabilized β-catenin may then accumulate in the cytoplasm and translocate to the nucleus, where it forms a complex with transcription factors TCF/LEF1 to promote the transcription of numerous *Wnt* target genes.

Crosstalk between the canonical *Wnt* pathway and other signaling pathways often occurs through GSK3β, a ubiquitously expressed serine/threonine kinase. GSK3β is one of two GSK3 isoforms (GSK3α and GSK3β). These isoforms arise from different genes, but they have 85% homology in their kinase domain. GSK3β is a hub protein that is involved in numerous pathways and cellular processes, including glucose metabolism as well as the canonical *Wnt*, Hedgehog, Notch and Receptor Tyrosine Kinase pathways [85].

GSK3β is expressed in all mammalian tissues, with especially high expression in the brain [87]. As a kinase, it is unusual in that it is very active in unstimulated somatic cells, and it is often through extracellular signals that its activity is reduced [88]. For example, stimulating cultured cells with insulin reduces GSK3β activity by 30-70% within a few minutes [89, 90]. Insulin signaling activates the PI3K pathway. AKT, a downstream effector of PI3K, subsequently phosphorylates GSK3β at Ser9, greatly reducing its activity. Integrin signaling through integrin linked kinase (ILK), growth factor signaling through Receptor tyrosine kinases (e.g. FGFR, EGFR, NGFR ect) , Ras and MAPK, and signaling through PKA can also induce Ser9 phosphorylation of GSK3β [91-94]. Though Ser9 phosphorylation is the most common or at least best characterized route to GSK3β inactivation, phosphorylation at other residues, including Thr43 and Ser389 through Erk and p38 MAPK signaling respectively also inhibits GSK3β activity [95,96]. Conversely GSK3β activity is increased upon auto-phosporylation or phosphorylation by ZAK1at Tyr216 [97].

GSK3β targets dozens of substrates for phosphorylation, often resulting in the inactivation of those substrates [98]. It plays a well-documented role in apoptosis pathways and cell cycle progression. Activated GSK3β negatively regulates the activity of prosurvival transcription factors like CREB and HIF-1

alpha, and it can form complexes with p53 in the nucleus to promote p53 mediated apoptosis [99, 100]. Small molecule inhibition of GSK3β promotes the survival of neural precursors and cardiac cells that have been deprived of serum or trophic factors [85]. Activated GSK3β phosphorylates the cell cycle regulator p27kip1, and in this case the phosphorylation results in increased stability of p27kip1,which then leads to cyclinD1 degradation and G1 cell cycle arrest [101]. Conversely GSK3β inhibition increases the stability of downstream phosphorylation targets such as c-myc and cyclinD1, promoting cell cycle progression and proliferation [98].

Though GSK3β participates in numerous signaling pathways, its involvement in the canonical *Wnt* pathway has perhaps received the most attention. The currently accepted model of canonical *Wnt* signaling does not explicitly require Ser9 phosphorylation and inactivation of Gsk3β. Nevertheless, Gsk3β inhibition by small molecule inhibitors is a commonly used method for activating canonical *Wnt* signaling *in vitro*. Numerous highly selective small molecule inhibitors of Gsk3β are commercially available, and their use is often more cost effective than recombinant *Wnt* proteins [102].

Gsk3β activity in PSCs appears to be species specific and depends on the differentiated state of the cell. Phoshoproteomic analysis of hESCs grown in a MEF conditioned medium revealed a high level of Tyr216 phosphorylation of GSK3β, indicating increased GSK3β activity [103]. Singh *et al*. reported that mESCs have a large fraction of inactivated GSK3β, while hESCs show a high level of GSK3β activity [104]. The authors argue that these differences in GSK3β activity reflect differing pluripotent states across species. mESCs are described as “naïve”, and the hESCs are described as “primed”. In the mESCs, reduced GSK3β activity is linked to the PI3K pathway, which promotes Ser9 phosphorylation of GSK3β, stabilizion of c-myc and Nanog and increased self renewal. On the other hand, in hESCs high GSK3β activity is linked to the inhibition of *Wnt*/β-catenin induced differentiation. When the hESCs were differentiated for 48 hours as EBs in serum containing medium, Ser9 phosphorylation of GSK3β increased substantially.

There is a great deal of controversy surrounding the role of canonical *Wnt* signaling in the regulation of hPSC self-renewal. A 2004 study by Sato *et al*. indicated that hESCs grown in unconditioned medium maintained high *Oct4* expression and undifferentiated colony morphology when

they were treated with a GSK3β inhibitor [41]. However more recent studies have cast doubt on those early results. Davidson *et al.* , for instance, argue that canonical *Wnt* signaling promotes differentiation, not self-renewal [105]. Similarly, Singh *et al*. found that GSK3β inhibition of hESCs encouraged mesendodermal differentiation in monolayer culture in manner that was concentration dependent [106]. The authors suggested that perhaps some of the confusion surrounding the canonical *Wnt* pathway's role in hPSC self-renewal arises because different research groups are using different concentrations of GSK3β inhibitors in their studies. At low doses, the hPSCs remain undifferentiated, but at higher doses, differentiation occurs. This is in agreement with Davidson, who reported that it took a concentration of 4 μM BIO to activate a *Wnt* reporter in hESCs [105]. By contrast, Sato *et al*. used 2 μM BIO in short-term experiments [41].

mTeSR1 contains 0.98 mM of the GSK3β inhibitor LiCl, but since very little nuclear localization of β-catenin is observed in hESCs grown in mTeSR1 under standard conditions, this concentration of LiCl appears to be too low to induce canonical *Wnt* signaling [107]. So what is the purpose of partial GSK3β inhibition if not to induce canonical *Wnt* signaling? The answer may have to do with the effect of GSK3β inhibition on the morphology of hPSC colonies grown in feeder free and feeder independent conditions. Differentiated fibroblastic cells are commonly found at the peripheries of hPSC colonies grown in MEF conditioned medium[108]. One group found that supplementing feeder free hESCs with 2.5 μM BIO led to an upregulation of E-cadherin and a decrease in the expression of markers of epithelial to mesenchymal transition (EMT) [109]. They observed a concomitant decrease in the number of fibroblastic/mesenchymal cells at the edges of the colony. Hence low concentrations of GSK3β inhibitors may promote epithelial morphology of hPSC colonies in the context of hPSC maintenance culture.

While the precise role of canonical *Wnt* signaling in hPSC pluripotency remains unresolved, its role in early embryonic development and PSC differentiation is well established. In mPSCs and hPSCs, *Wnt/* β-catenin signaling cooperates with the Activin and BMP pathways to induce mesendodermal differentiation [110]. High concentrations of the GSK3β inhibitor BIO in unconditioned hESC medium induce Brachyury, an early mesendodermal marker, in hESCs in monolayer culture. Brachyury expression in early mouse and zebrafish embryos has been linked to canonical *Wnt* signaling, and Brachyury is a direct

target of β-catenin in mESCs [111]. In the absence of Activin/Smad signaling, however, canonical *Wnt* signaling promotes neural crest fate [112]. When β-catenin is knocked out, mESCs showed a complete lack of mesendodermal differentiation [113]. β-catenin -/- mESCs generate EBs that are smaller than wild type EBs and present defects in cell-cell adhesion, specifically persistent E-cadherin expression.

1.7 E-Cadherin and Epithelial to Mesenchymal Transitions in hPSC Maintenance and Differentiation

Undifferentiated hPSCs are largely E-cadherin positive, as are human oocytes and preimplantation embryos [114-116]. In fact its expression in hPSCs is so pervasive that some researchers have proposed using it as a marker of pluripotency [114]. hPSCs have low viability when dissociated into single cell suspensions, and this sensitivity to dissociation has been linked to loss of E-cadherin signaling[117,118].

Intact E-cadherin signaling is also crucial during the initial stages of EB formation and culture. Incubating floating mESC and hESC aggregates with an anti-E-cadherin antibody prevents EB formation [116]. But as cells within EBs differentiate, the initially very high E-cadherin expression gradually decreases and in some cases, becomes localized to a squamous epithelial layer located on the outside layers of the EB [113, 116, 119, 120].

E-cadherin is coupled to the actin cytoskeleton by a protein complex that includes p120 catenin, β-catenin and α-catenin [121]. Together these proteins comprise an “adherens junction”. Formation and turnover of adherens junctions can influence intracellular signaling events [122]. For example, in addition to participating in the formation of adherens junctions, β-catenin is a crucial effector protein in the canonical *Wnt* pathway. Studies of other cell types suggest that the β-catenin found in adherens junctions and the β-catenin that participates in *Wnt* signaling come from the same pool [123]. Thus E-cadherin signaling can sequester β-catenin at the cell membrane, leaving it unavailable to participate in canonical *Wnt* signaling.

Loss of E-cadherin is characteristic of an epithelial to mesenchymal transition (EMT). In cells undergoing EMT, transcriptional repressors of E-cadherin repressors like Snail, Slug and Twist are up

regulated, resulting in a mesenchymal phenotype, resistance to anoikis, loss of cell polarity and increased expression of other cell adhesion molecules such as N-cadherin and NCAM1 [124].

EMTs occur several times during embryological development, notably during gastrulation and neural crest development. The canonical *Wnt*, TGFβ, FGF and EGF signaling pathways can all induce EMT [83]. *PSCs* in both the mouse and human model show signs of EMT during differentiation, and differential expression of cell adhesion molecules can mark the appearance of various differentiated phenotypes [114, 125]. For example, cells in the neural plate arising from embryonic ectoderm down regulate E-cadherin and express N-Cadherin[126]. N-cadherin is present in *in vitro* derived neural rosettes as well as mesendodermal tissues that emerge during gastrulation [127, 128]. NCAM1 is often used as a marker for the isolation of hPSC derived neurons, though it is also expressed in a population of $NCAM1^{+}$ / $CD326^{-}$ hPSC derivatives that give rise to mesoderm *in vitro* [129,130].

GSK3β has been shown to regulate EMT in some cell types. Activated GSK3β phosporylates and decreases the half life of Snail, a well known mediator of EMT [131]. Upon GSK3β inhibition, Snail is stabilized and binds to the E-cadherin promoter, inhibiting its transcription. One group has found that GSK3β inhibition results in a transcriptional up regulation of Snail as well as stabilization at the protein level [132]. Other members of the Snail family of transcription factors like Slug and the Twist family of transcription factors are also targets of GSK3β phosphorylation and destabilization in drosophila [123,133]. Interestingly FGF signaling can induce EMT via phosphorylation of GSK3β at Ser9 through PI3K/AKT, and the inactivation of GSK3β can lead directly to stabilization of Snail [134].

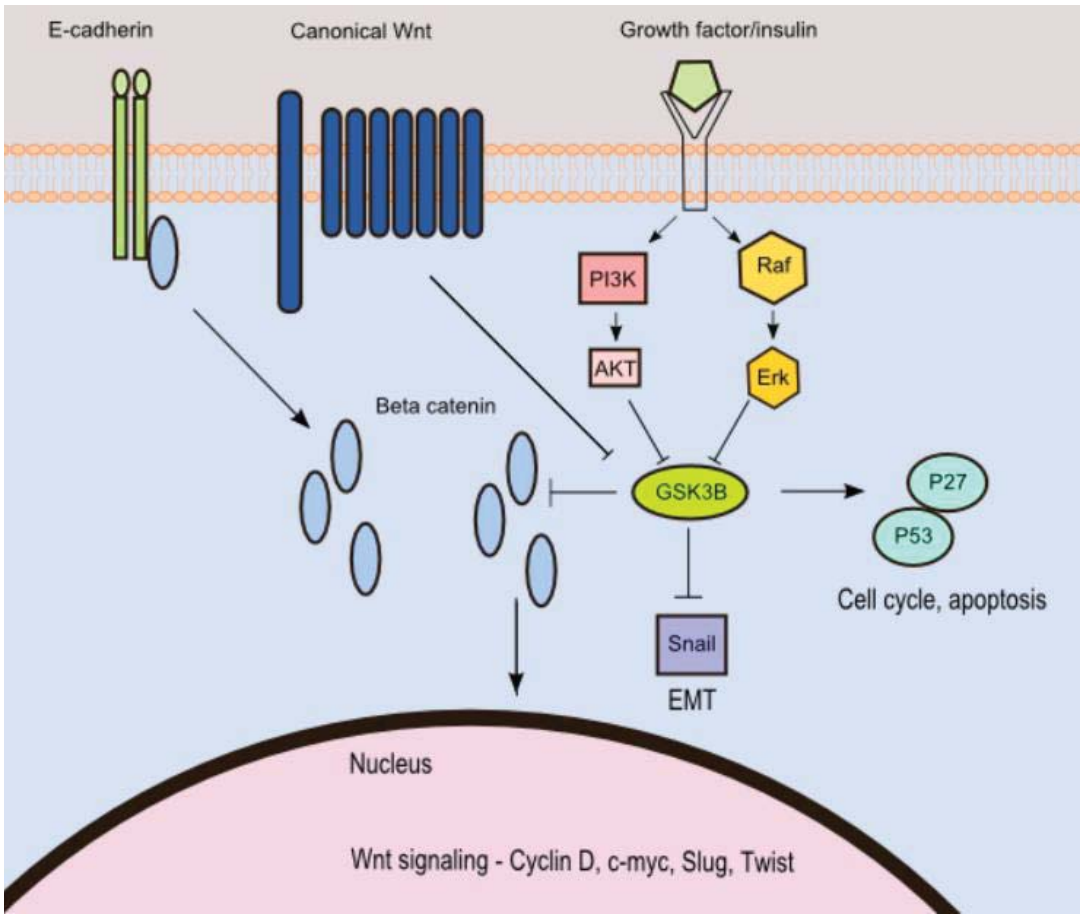

Figure 1.2 **Cross talk between growth factor, canonical *Wnt* and cell-cell signaling through GSK3β and β-catenin.**

1.8 Project rationale and hypothesis

It is common to add bFGF to EBs generated from hPSCs adapted to mTeSR1. Given that GSK3β is a downstream target of growth factor signaling and that Ser9 phosphorylation of GSK3β often accompanies hPSC differentiation in the EB model, we propose that partial inhibition of GSK3β is sufficient to promote the survival, growth and early development of EBs. In order to investigate this hypothesis, we will develop a serum free EB medium that is compatible with mTeSR1adapted hPSCs. We will generate three groups of EBs in this medium and compare them in terms of growth, survival, differentiation, proliferation and patterns of cell-cell interactions. The three groups are: a control group of EBs fed only a basal EB medium, a group supplemented with bFGF, and a group supplemented with a small molecule inhibitor of GSK3β.

Chapter 2 – MATERIALS AND METHODS

2.1. hESC culture

H9 human embryonic stem cells (Wicell) were maintained in a mTeSR1 medium (Stem Cell Technologies) according to the manufacturer's recommendations. Briefly, H9s (P48-P57) were seeded onto Matrigel coated (BD Biosciences) tissue culture polystyrene dishes. Medium was exchanged every day, and cells were passaged every 3-4 days at a split ratio of 1:4 -1:5. Colonies were examined under an inverted phase contrast microscope for signs of differentiation before passaging, and colonies that appeared differentiated were removed by scraping with a plastic pipette tip. Cells were passaged using a combination of enzymatic and mechanical dissociation. Cells were incubated in 1 mg/ml dispase (Stem cell Technologies 07923) for 7 min or until the edges of the colonies began to curl. The dispase was then aspirated and the colonies were rinsed three times in DMEM/F12. Enough mTeSR1 to cover the cells was added, and a glass 5 ml pipette was used to scrape the colonies off the surface of the dish. The suspension of cell aggregates was transferred to a 15 ml centrifuge tube. The colonies were broken into smaller pieces by pipetting up and down several times with a 5 ml glass pipette. The appropriate volume of medium was added, and the cell aggregates were transferred to new Matrigel coated dishes. The dishes were inspected under an inverted phase contrast microscope to ensure that the aggregates were the appropriate size (~50-100 μm in diameter). The dishes were placed in a 37° C incubator with 5% CO_2.

2.2 SF- EB medium

A mTeSR1 compatible medium was assembled using the ingredients listed in **Table 2.1**.

Table 2.1. Formulation of a mTeSR1 compatible EB medium.

Component	1x concentration	Vendor	Catalog Number
DMEM/F12	79.3%	Hyclone	SH30261.01
Bovine Serum Albumin	12.96 mg/ml	Sigma Aldrich	A9418
Insulin	20 μg/ml	Gibco	41400-05
Transferrin	10 μg/ml	Gibco	41400-05
Glutamax	1 mM	Gibco	35050-061

β-mercaptoethanol	0.1 mM	EMD Millipore	ES-007-E
Non-Essential Amino Acids	1%	Hyclone	SH30238.01
Trace Elements B	0.20%	Cellgro	99-175-C1
Trace Elements C	0.10%	Cellgro	99-176-C1
Chemically Defined Lipids	0.00195 ml/ml	Gibco	11905-031
Na-Selenite	0.0306 µg/ml	Sigma Aldrich	S5261
Reduced Glutathione	1.96 µg/ml	Sigma Aldrich	G4251
Ascorbic Acid	45 µg/ml	Sigma Aldrich	A4544
Thiamine HCl	8.16 µg/ml	Sigma Aldrich	T1270
Sodium bicarbonate	0.544 mg/ml	Sigma Aldrich	S7277
NaCl	1.89 mg/ml	Acros	327300010

2.3 SF-EB Formation Protocol

To form EBs, H9 cells were first cultured in 100 mm dishes (Corning 430167) to 70-90 % confluence. EBs were formed as described previously with modifications [135]. Briefly, the cells were incubated at 37° C with 0.5 mg/ml dispase (Stem cell Technologies 07923) in DMEM/F12 for 30-40 min, or until the colonies began to lift off of the plate. The plates were gently shaken to help dislodge the colonies. No mechanical scraping was used to dislodge the colonies. The dispase solution was diluted in DMEM/F12 and the suspension was transferred to a 15 ml centrifuge tube. The cell aggregates were allowed to settle by gravity, and the dispase solution was gently aspirated. The aggregates were washed three more times in DMEM/F12 before being resuspended in 12 ml of SF-EB medium. The suspension was gently pipetted up and down to mix and 2 ml of medium/cell suspension was transferred to each well of a 6 well ultra-low attachment plate (Costar 3471). A portion of 1 ml of SF-EB medium was then added to each well to bring the total volume per well to 3 ml. Some SF-EBs were fed with growth factors or chemical inhibitors (See section **2.4**). The SF-EBs were cultured in suspension with 2/3 medium exchanges on day 1 and day 3. SF-EBs were collected for analysis 2 and 5 days after being placed in suspension.

2.4 Treatments

Some SF-EB groups were treated with growth factors or small molecule inhibitors. Human bFGF (Peprotech 100-18B) was aliquoted in Tris-HCl (1 M, pH 7.5) to a concentration of 100 mg/ml and then

further diluted to 10 mg/ml in 1% BSA. SF-EBs were treated with 10 ng/ml bFGF. The GSK3β inhibitor 6-Bromoindirirubin-3' oxide (BIO) (Sigma Aldrich B1686) was obtained from Sigma Aldrich and aliquoted in DMSO to a stock concentration of 500 μM. SF-EBs were treated with BIO at a concentration between 100-1000 nM. Working solutions were stored at -20° C.

2.5 Microscopy

SF-EBs were examined daily under an inverted microscope and brightfield microscopy images were taken on day 2-5 of the experiments using an Olympus IX71 inverted microscope and Slidebook software. SF-EB diameters were determined using the Slidebook Imaging Analysis software.

2.6 Cell Counting

On days 2 and 5 of the experiment, SF-EBs were transferred to 15 ml tubes, rinsed with PBS, and incubated in prewarmed Accutase (Stem cell Technologies 7920) for 5 min at 37° C. The suspension was then pipetted up and down several times with a P1000 micropipette tip to produce a single cell suspension. A portion of 3 ml of SF-EB medium were added to the single cell suspension to dilute the accutase, and the tubes were centrifuged. The accutase was aspirated and the cells were resuspended in SF-EB medium to an estimated density of 10^6 cells/ml. 20 μl of cell suspension was mixed with 20 μl of trypan blue dye. 10 μl of solution was transferred to a hemacytometer (Hausser Scientific 3120), and the 4 corners were counted. Cells per milliter were calculated with the following equation:

$$\frac{\#\text{ of cells}}{\#\text{ of squares counted}} \times \text{Dilution} \times \text{Volume of Cell Suspension} \times 10{,}000$$

2.7 Quantitative Real Time PCR (qRT-PCR)

RNA was extracted from SF-EBs using a RNeasy minikit from Qiagen (74134). RNA concentration was determined using a Biotek Synergy Mx spectraphotometer with a Gen 5 Take 3 module. Ratios of absorbance at 260 and 280 nm were measured to determine the purity of the RNA. Reverse transcription (RT) was carried out using Applied Biosystems High Capacity cDNA reverse transcription kit (4368814) using the manufacturer's protocol. qRT-PCR was carried out using the Power

SYBR Green PCR Master Mix (Applied Biosystems 4368708). All components were kept on ice when not in use. The reactions were carried out on an Eppendorf realplex4. Fold change calculations were performed using the ΔΔCt method. The housekeeping gene was Beta actin. Undifferentiated H9 hESCs were used as controls. See Appendix for detailed protocols. Primers used for qRT-PCR are listed in **Table 2.2**.

Table 2.2 Primers for qRT-PCR.

	Forward	Reverse	Product length
Oct 4	TGGGCTCGAGAAGGATGTG	GCATAGTCGCTGCTTGATCG	78
Nanog	AGAAGGCCTCAGCACCTAC	GGCCTGATTGTTCCAGGATT	206
E-Cadherin	CGAGAGCTACACGTTCACGG	GGGTGTCGAGGGAAAAATAGG	119
N-Cadherin	ATCGAAGGATGTGCATGAAG	GCATGCTCAGAAGAGAGTGG	165
NCAM1	CCTCCACCCTCACCATCTAT	AGCTGACCACATCACACACA	198
Twist	CATCCTCACACCTCTGCATT	TGATGCCTTTCCTTTCAGTG	153
Slug	CTGCAGACCCATTCTGATGT	GCTACACAGCAGCCAGATTC	107
Snail	TCGGAAGCCTAACTACAGCGA	AGATGAGCATTGGCAGCGAG	140
Brachyury	CTATTCTGACAACTCACCTGCAT	ACAGGCTGGGGTACTGACT	146
Sox17	CAAGGGCGAGTCCCGTATC	GCCCAGCATCTTGCTCAACT	124
NeuroD1	AAGAACTACATCTGGGCTCTGT	GTGGTGGGTTGGGATAAGC	104
β-Actin	ATCCACGAAACTACCTTCAACTC	AGGGCAGTGATCTCCTTCTG	140

2.8 Immunostaining

EBs were fixed in 4% paraformaldehyde (Sigma Aldrich P6148) for 20 min. Then they were incubated at room temperature in a 7.5% Sucrose (Fluka 84097) solution in PBS for 3 h. Next, the EBs were incubated with a 15 % sucrose solution in PBS overnight at 4° C. The EB/Sucrose solution was transferred to a 15X15X5 mm vinyl freezing medium mold (Tissue Tek). The sucrose solution was carefully aspirated, and enough freezing medium was added to fill the mold. The molds were frozen at -20 ºC and then either stored at –80ºC or used immediately for cryosectioning. 8 µm sections were generated using the Triangle Biomedical Systems Minotome Plus. The sections were transferred to poly-L-lysine coated slides (Electron Microscopy Sciences #63410) and stored at -80ºC until ready for use. Slides were blocked in 1% BSA in PBST for 30 min. Antibodies were diluted in 1% BSA in PBST. The following primary antibodies and dilutions were used: mouse monoclonal anti-E-cadherin 1:200 (Abcam 1416), rabbit monoclonal anti-β-catenin (dilution ration: 1:100) (Abcam 32572), rabbit polyclonal anti-Collagen IV (dilution ratio: 1:100) (Abcam 6586). Samples were incubated with primary antibody at room

temperature for 1 h. The following secondary antibodies were used: Dylight 488 conjugated goat anti-mouse IgG (dilution ratio:1:200) (Thermo Scientific 35503), TRITC-conjugated Affinipure Donkey Anti-rabbit IgG (dilution ratio:1:200) (Jackson Immuno Research 711-025-152). Samples were incubated with secondary antibody for 1 h in the dark. Samples were counterstained with DAPI (Invitrogen) for 1 min in the dark. See Appendix for detailed protocols.

2.9 Western Blot

SF-EBs were transferred to eppendorf tubes and rinsed with PBS. Samples were frozen at -80°C until ready for lysing. Samples were lysed in RIPA lysis buffer. The samples were denatured in loading buffer at 95°C for 10 min. The proteins were resolved by 10% SDS-PAGE. The molecular weight markers used were Pageruler Plus Prestained Protein Ladder (Thermo Scientific 26619). Wet transfer was done using a nitrocellulose membrane (BIO-RAD 1101093).

The membrane was blocked using 5% milk in PBST for 1 h at 25°C. The primary antibody was diluted in a blocking buffer. Samples were incubated overnight at 4°C. The membrane was washed 3x times with PBST. The membrane was then incubated with HRP-conjugated secondary antibody in PBST at room temperature under constant agitation for 1 h. The samples were developed using the SuperSignal West Pico Chemiluminescent Substrate (Thermo Scientific 34077). Images were taken using the BIO Rad Universal Hood II.

Anti-Beta Catenin Rabbit monoclonal antibody (Abcam ab32572) was used at 1:5000 dilution. Beta actin HRP-conjugated antibody (Sigma Aldrich A3854) was used as a loading control. Goat polyclonal anti rabbit conjugated to HRP (Rockland 611-1302) was used as a secondary antibody. See Appendix for detailed protocols.

2.10 Statisical Analysis

Single factor Analysis of Variance was performed with Tukey-Kramer Post-Hoc Analysis. In some cases, two tailed student's t-tests were performed to obtain p values. Statistical significance was set to $p<0.05$.

Chapter 3 - Results

3.2 EB formation in a mTeSR1 compatible serum-free medium

First, we investigated the effect of EB medium composition on the efficiency of EB formation. H9 hESCs were grown on Matrigel coated plates and maintained in mTeSR1. When the cultures reached approximately 70% confluency, they were incubated with 0.5 mg/ml dispase to dislodge them from the plate, and the largely intact colonies were rinsed, resuspended and transferred to ultra low attachment dishes. EBs would form within 24-48 h.

The efficiency of EB formation depended on the composition of the EB medium that the putative EBs were fed. When EBs were formed in a medium containing knockout serum replacement (KOSR) (**Table 3.1)**, a proprietary serum replacement commonly used in the maintenance of feeder dependent hPSCs, a large amount of cell debris and cell death was observed (**Fig. 3.1**) . We hypothesized that the low efficiency of EB formation observed in a KOSR containing medium was due to medium incompatibility and that EB formation from mTeSR1 adapted hPSCs could be improved if the EB medium was more similar to mTeSR1 in its composition. To validate this hypothesis, we developed an EB formation medium (**Table 3.2**) based on the published formulation of mTeSR1. This EB medium is serum-free and contains all of the components of mTeSR1 except for the pluripotency factors (i.e. bFGF, TGFβ1, LiCl, GABA and pipecolic acid). For clarity, this mTeSR1 based medium will hereafter be referred to as "serum-free EB (SF-EB) medium" and EBs cultured in this medium will be referred to as SF-EBs.

Table 3.1 EB medium containing Knockout Serum Replacement

Component	1x concentration	Vendor	Catalog Number
DMEM/F-12 w/ L-glutamine	78%	Hyclone	SH30261.01
Knockout serum replacement	20%	Invitrogen	10828-028
β-mercaptoethanol	0.1 mM	EMD Millipore	ES-007-E
Non-Essential Amino Acids	1%	Hyclone	SH30238.01

Table 3.2 SF-EB medium

Component	1x concentration	Vendor	Catalog Number
DMEM/F12 w/ L-glutamine	79.3%	Hyclone	SH30261.01
BSA	12.96 mg/ml	Sigma Aldrich	A9418
Insulin	20 µg/ml	Gibco	41400-05
Transferrin	10 µg/ml	Gibco	41400-05
Glutamax	1%	Gibco	35050-061
β-mercaptoethanol	0.1 mM	EMD Millipore	ES-007-E
Non-Essential Amino Acids	1%	Hyclone	SH30238.01
Trace Elements B	0.20%	Cellgro	99-175-C1
Trace Elements C	0.10%	Cellgro	99-176-C1
Chemically Defined Lipids	0.00195 ml/ml	Gibco	11905-031
Na-Selenite	0.0306 µg/ml	Sigma Aldrich	S5261
Reduced Glutathione	1.96 µg/ml	Sigma Aldrich	G4251
Ascorbic Acid	45 µg/ml	Sigma Aldrich	A4544
Thiamine HCl	8.16 µg/ml	Sigma Aldrich	T1270
Sodium bicarbonate	0.544 mg/ml	Sigma Aldrich	S7277
NaCl	1.89 mg/ml	Acros	327300010

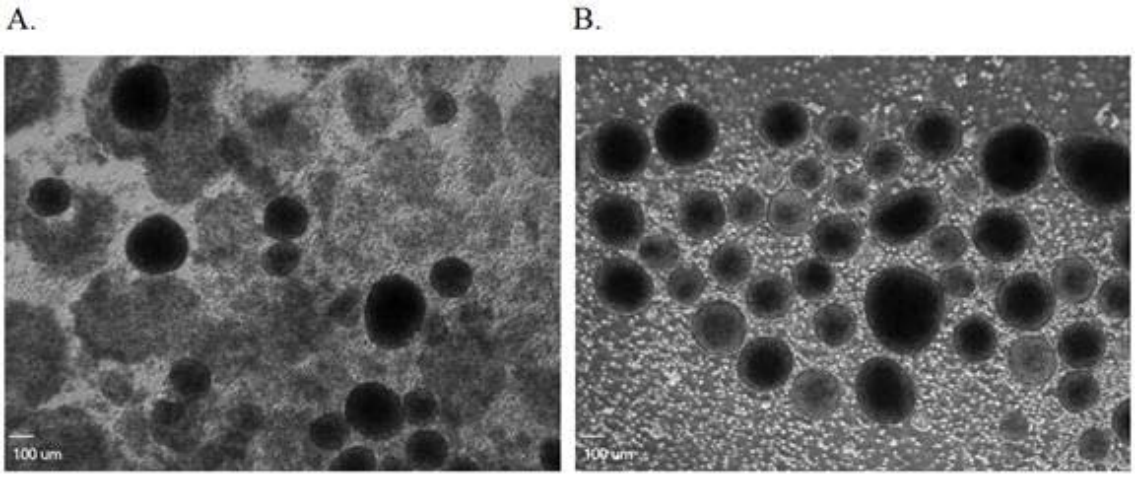

Figure 3.1. Micrographic images of EBs derived from H9 hESCs two days after formation. (A) EBs in KOSR containing medium. (B) EBs in mTeSR1 compatible SF-EB medium.

Unlike EBs formed in KOSR containing medium, SF-EBs formed in SF-EB medium appeared healthy, and far less cell debris was observed during initial EB formation, suggesting a higher cell survival rate (**Fig 3.1B**). The SF-EB medium was used for all subsequent experiments.

3.3 Without growth factor supplementation, SF-EBs tend to degrade in extended culture

Even though SF-EBs formed readily in SF-EB medium, they tended to degrade after a few days in suspension culture. SF-EBs generated from both H9 hESCs and IMR90 hiPSCs, which had had been largely round and symmetrical two days after SF-EB formation, began losing their characteristic round shape starting on days 3-4 (**Figure 3.2 B-C**), and we observed increased amounts of cell debris in the wells. By day 5 of suspension culture, most of the SF-EBs that had been fed the basal SF-EB medium (hereafter called "control SF-EBs") had become irregularly shaped or were falling apart.

3.4 Treatment with bFGF or small molecule inhibitors of GSK3β promotes improved SF-EB morphology and growth.

It has been previously reported that treating EBs derived from mTeSR1 adapted cultures with bFGF improves EB survival in suspension culture [72]. In order to investigate the effects of bFGF and GSK3β inhibition on the development of SF-EBs, SF-EBs were generated in SF-EB medium (control), SF-EB medium supplemented with 10 ng/ml bFGF or SF-EB medium supplemented with 300 nM of the GSK3β inhibitor BIO. The SF-EBs were cultured in suspension for 5 days with medium refreshment every other day.

After two days in suspension, we observed no significant difference between any of the three treatment groups in terms of mean SF-EB diameter, viable cells per well or morphology. However, as shown in **Fig. 3.2**, **Fig. 3.3** and **Fig 3.4**, the SF-EBs showed great sensitivity to growth factor stimulation and BIO treatment at later time points. On day 5 of suspension culture, both the bFGF and BIO treated SF-EBs had significantly larger average diameters and higher cell counts per well than untreated control SF-EBs. Interestingly, even though the bFGF and BIO treated SF-EBs' did not differ significantly in terms of mean SF-EB diameter (**Fig 3.3**), bFGF treated SF-EBs did have a significantly higher viable cell count per well than BIO treated SF-EBs, suggesting that cell density and proliferation rates were higher in bFGF treated SF-EBs than BIO treated SF-EBs.

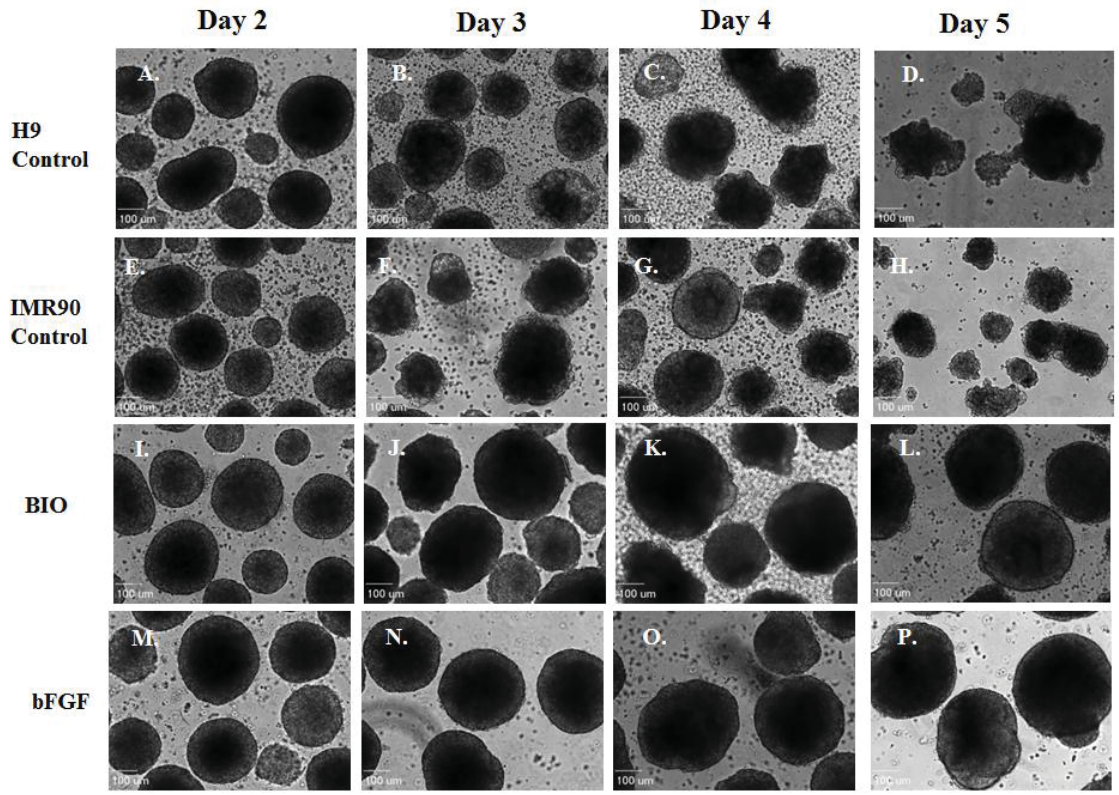

Figure 3.2. Morphologies of hPSC-derived SF-EBs cultured under different conditions at different time points. (A-D) H9 derived EBs cultured in SF-EB medium. (E-H) IMR90 hiPSC derived EBs cultured in SF-EB medium. (I-L) H9 derived EBs cultured in SF-EB supplemented with GSK3β inhibitor BIO (300 nM) (M-P)) H9 derived EBs cultured in SF-EB supplemented with 10 ng/ml bFGF.

Treatment with either bFGF or BIO resulted in a more spherical morphology in SF-EBs compared to untreated controls, though the morphologies of BIO treated SF-EBs were slightly more heterogeneous than the bFGF treated SF-EBs. And BIO treatment, despite promoting cell proliferation overall, did not prevent the accumulation of some cell debris in some experiments, an effect not observed in bFGF treated SF-EBs.

The effect of BIO was also strongly dose dependent. While treatment with 300 nM BIO was sufficient to maintain SF-EB morphology and growth as compared to controls, increasing the concentration of BIO to 500 nM resulted in widespread SF-EB agglomeration (**Fig. 3.5).** This agglomeration produced very large cellular aggregates. Such large agglomerations of SF-EBs would likely limit oxygen and nutrient transport into the interior of the aggregates. Thus 300 nM BIO was used for most experiments. Interestingly, the concentration of BIO used in our experiments (300 nM) was considerably lower than the concentrations other groups have reported as being necessary for the activation of canonical *Wnt* signaling in hPSCs in monolayer culture [41, 106].

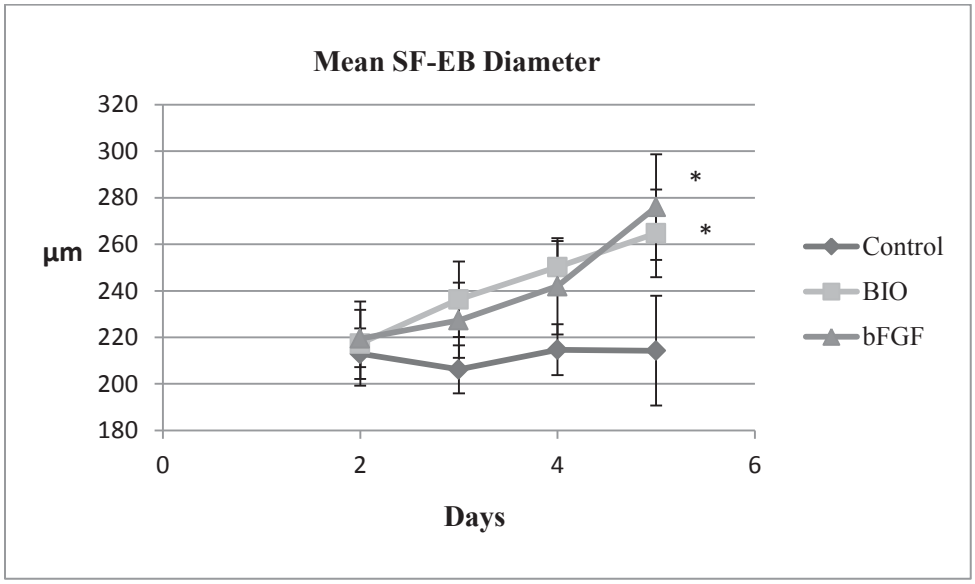

Figure 3.3. Mean SF-EB diameter 2 and 5 days after EB formation (n=8). EBs were generated from mTeSR1 adapted cultures and grown in suspension for 5 days. Some SF-EBs were treated with BIO (300 nM) or bFGF (10 ng/ml). SF-EB diameters were determined via brightfield images analyzed with Slidebook software. Average values are calculated from measurements of 20 randomly chosen SF-EBs from each treatment group. * $p<0.05$ compared to control SF-EBs on day 5.

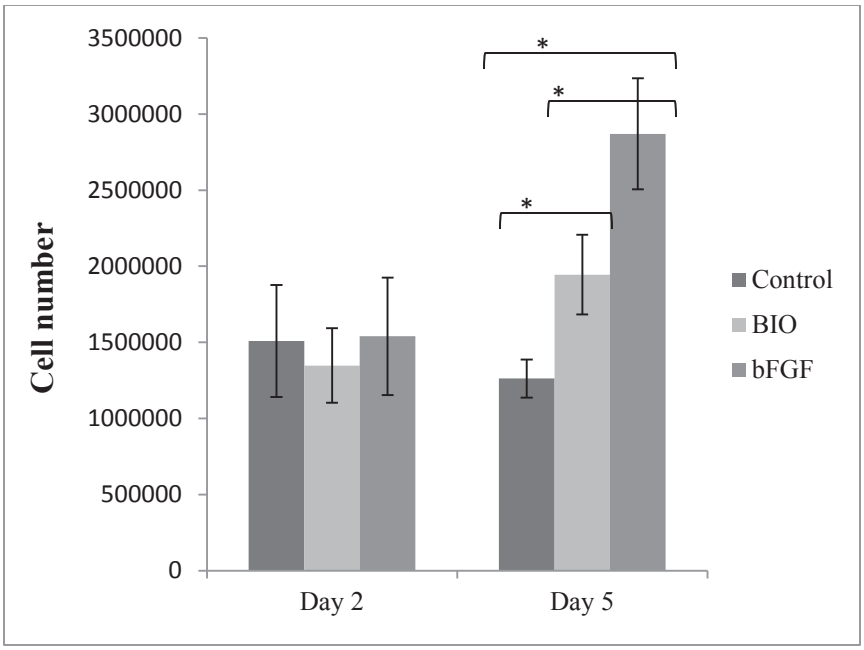

Figure 3.4. Proliferation of cells in EBs performed 2 and 5 days after formation. Control EBs were grown in suspension in SF-EB medium. BIO and bFGF EBs were grown in suspension in SF-EB medium plus 300 nM BIO or 10 ng/ml bFGF respectively. The data represents the average of three independent experiments (n=3). Error bars represent standard deviation. * indicates $p<0.05$ by single factor ANOVA.

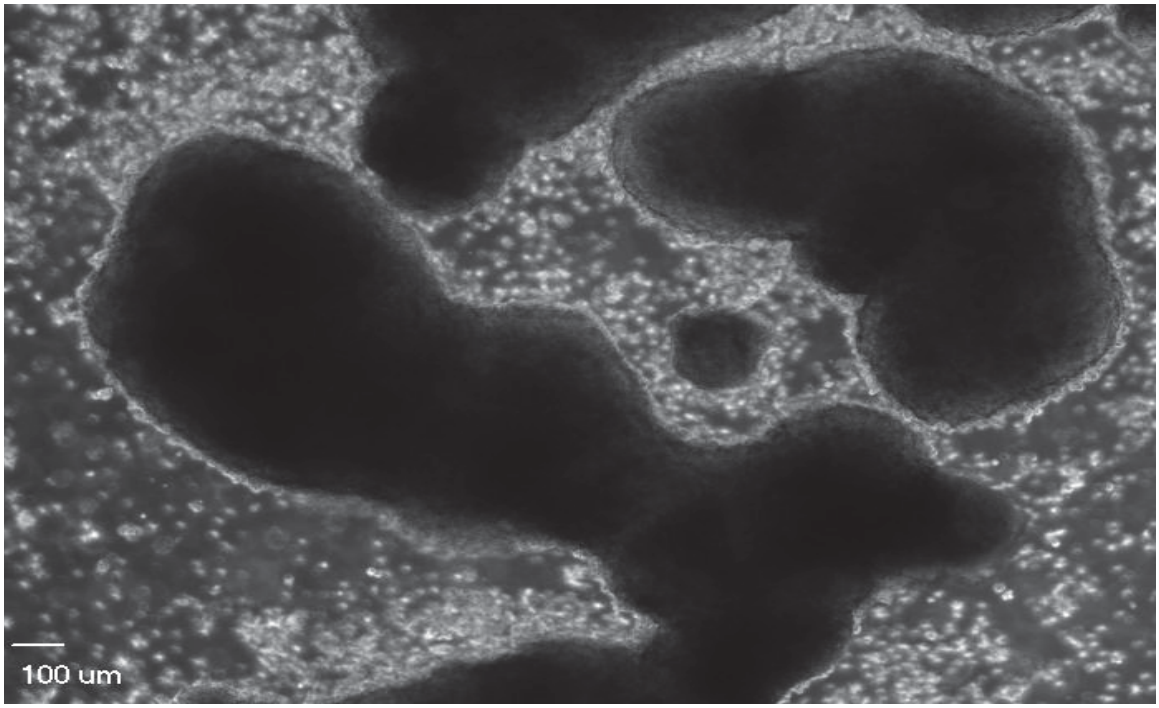

Figure 3.5. Agglomeration of SF-EBs at day 5 post EB formation in the presence of 500 nM BIO. Scale bar = 100 µm.

3.5 Cell-cell signaling within SF-EBs cultured under different conditions

We next hypothesized that the observed differences in SF-EB development as the result of different bFGF or BIO treatment are correlated with differential expression of proteins associated with cell adhesion. In order to test this hypothesis, we evaluated E-cadherin and β-catenin expression in SF-EBs using immunostaining, qRT-PCR and western blot.

On day 2 or day 5 after SF-EB formation, SF-EBs were cut into 8 μm-thick sections using a cryotome, placed on poly-L-lysine coated slides and subjected to immunofluorescence staining. As shown in **Fig 3.6A**(a-f), on day 2, E-cadherin and β-catenin were expressed throughout the SF-EBs regardless of treatment, and the findings were confirmed for E-cadherin by qRT-PCR (**Fig3.6C).** These results indicate that bFGF or BIO treatment of the SF-EBs had no apparent effect on the patterns of cell-cell signaling at day 2 and that cell-cell signaling within day 2 SF-EBs from all three treatment groups is dominated by E-cadherin, much as in undifferentiated hPSCs. The colocalization of β-catenin with E-cadherin may indicate that β-catenin is participating primarily in cell-cell signaling rather than canonical *Wnt* signaling at this time point. These patterns of cell-cell signaling coincide with the similar morphologies observed in SF-EBs in all treatment groups at day 2.

However, differences in cell-cell signaling between the different treatment groups had become apparent by day 5 post SF-EB formation. E-cadherin expression remained high in day 5 control SF-EBs (**Fig. 3.6A(g)**). On the other hand, SF-EBs that had been treated with either 10 ng/ml bFGF or 300 nM BIO showed evidence of decreased E-cadherin expression at the protein level (**Fig. 3.6A(h-i)**). In day 5 bFGF or BIO treated SF-EBs, E-cadherin tended to be localized to the outside of the EBs. Some BIO treated SF-EBs showed reduced E-cadherin expression, but with random localization (**Fig3.6B)**. On day 5, there was no indication that control SF-EBs were down regulating E-cadherin. The differences in E-cadherin expression on day 5 between the different treatment groups was confirmed by qRT-PCR (**Fig 3.6D**). Strangely the E-cadherin mRNA expression in control SF-EBs was very high even compared to undifferentiated H9s, which themselves express high levels of E-cadherin [116].

In control SF-EBs, β-catenin expression remained high on day 5, appearing to colocalize with E-cadherin. Some BIO treated samples showed β-catenin expression throughout the interior of the SF-EB, indicating the presence of β-catenin in the cytoplasm and perhaps the nucleus (**Fig 3.6A(h) and Fig3.6B**). The bFGF SF-EBs, on the other hand, show an overall reduction in β-catenin expression in the areas of the SF-EB where E-cadherin expression is also reduced. Western blot analysis of whole cell lysates from day 5 SF-EBs indicates that β-catenin levels are reduced in bFGF treated SF-EBs compared to controls and BIO treated SF-EBs (**Fig 3.7**).

Reduced E-cadherin is associated with epithelial to mesenchymal transitions (EMTs) and hPSC differentiation more generally [114]. E-cadherin down regulation as a result of EMT is often accompanied by up regulation of other cell adhesion molecules such as N-cadherin and NCAM1. qRT-PCR shows that N-cadherin and NCAM1 are up regulated in BIO and bFGF treated SF-EBs compared to control SF-EBs after 5 days in suspension (**Fig3.6D**).

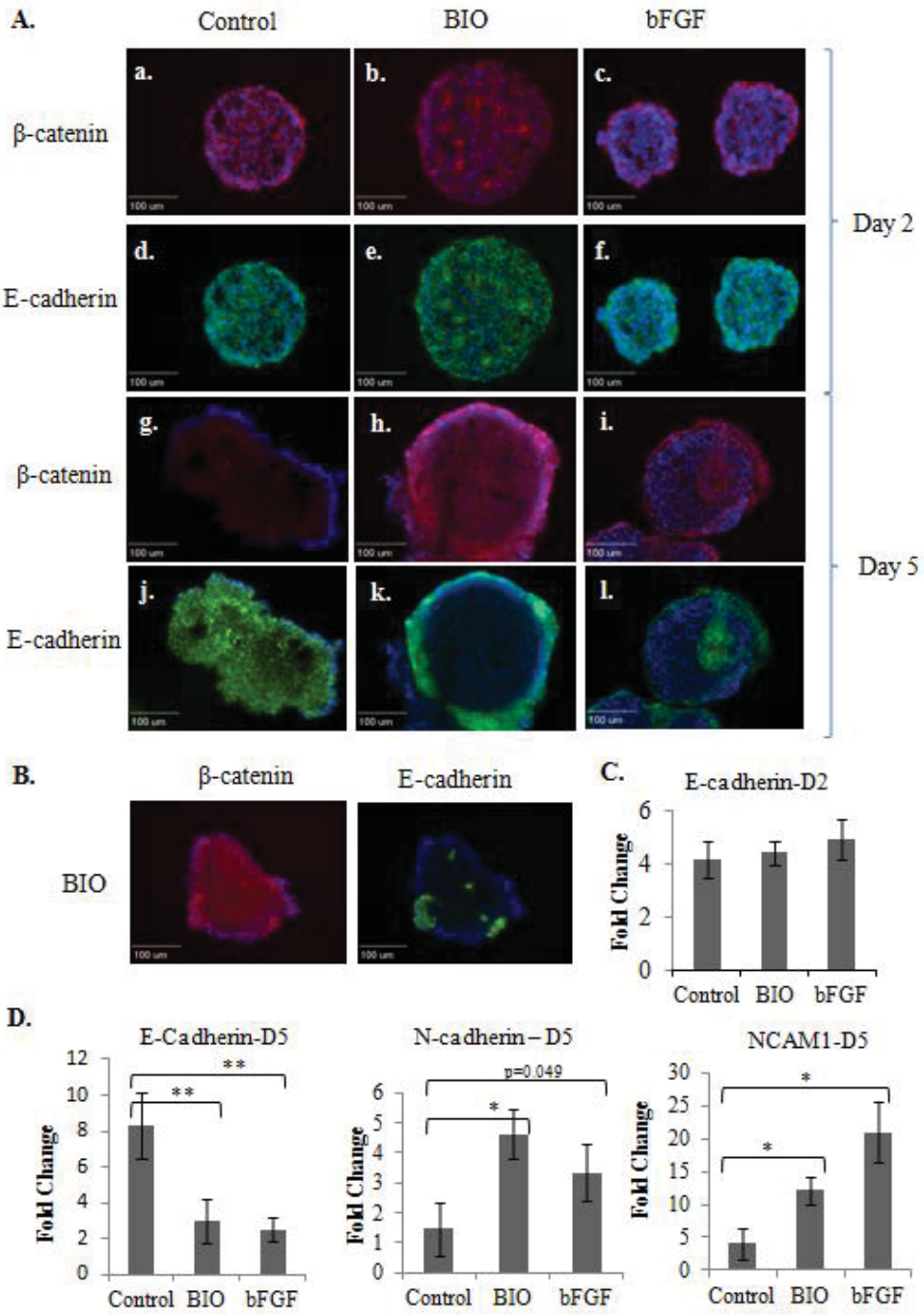

Figure 3.6. Cell-cell adhesion in SF-EBs. (A) Representative immunostaining results for β-catenin and E-cadherin expression in day 2 (a-f) and day 5 (g-l) SF-EBs cultured in SF-EB medium (Control), SF-EB medium with 300 nM BIO or SF-EB medium with 10 ng/ml bFGF. Cells were counter-stained with DAPI. Scale bar = 100 μm. (B) β-catenin and E-cadherin localization in some 300 nM BIO treated SF-EBs on day 5. (C) qRT-PCR results for E-cadherin expression in day 2 EBs. (n=1). (D) qRT-PCR results for cell adhesion molecules in differentiating day 5 SF-EBs (n=3). * indicates $p<0.05$ and ** indicates $p<0.01$ by single factor Anova. Fold changes were calculated relative to undifferentiated H9s. β-actin was used as

a housekeeping gene. p value in N-cadherin results calculated by two tailed student's t-test. Error bars represent standard deviation.

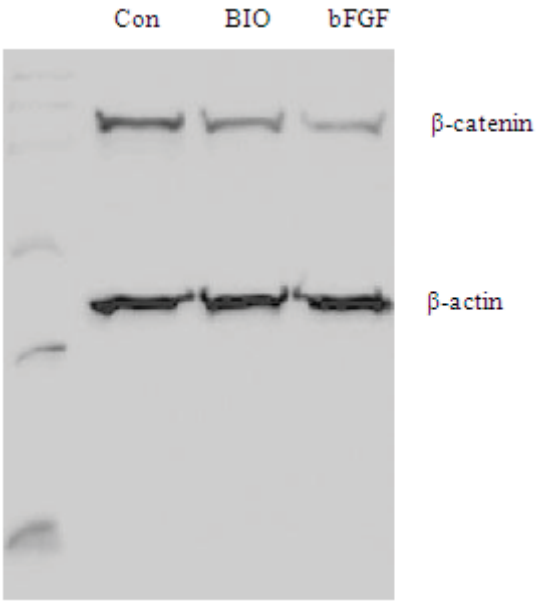

Figure 3.7. Western blot results for β-catenin expression in day 5 SF-EBs cultured in SF-EB medium (Control), SF-EB medium with 300 nM BIO or SF-EB medium with 10 ng/ml bFGF. β-actin was used as a loading control. (n=1).

Since transcription factors from the Snail and Twist family are known to inhibit the mRNA expression of E-cadherin, we hypothesized that bFGF and BIO treated SF-EBs would have increased mRNA expression of Snail, Slug and Twist1compared to control SF-EBs. However qRT-PCR analysis of Snail Slug and Twist1 expression in day 5 SF-EBs did not reveal a statistically significant difference between treatment groups as determined by a two-tailed student's t-test or single factor Anova (**Fig3.8**).

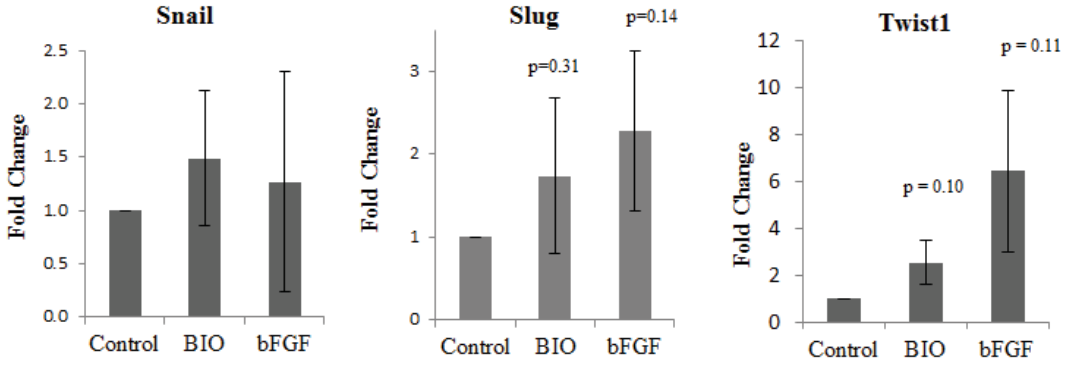

Figure 3.8. qRT-PCR analysis of Snail (n=2), Slug and Twist1 (n=3) in SF-EBs at day 5. Fold changes are determined relative to day 5 control SF-EBs. Error bars indicate standard deviation. p values are determined by two tailed student's t-test compared to Day 5 control SF-EBs.

3.5 Germ Layer Marker Expression in SF-EBs

One of the key developmental events commonly observed in EBs is the gradual reduction of pluripotency marker expression and differentiation into cells from the three germ layers. We evaluated pluripotency and germ layer expression in day 2 and day 5 SF-EBs fed SF-EB medium alone (control), or SF-EB medium supplemented with either 300 nM BIO or 10 ng/ml bFGF.

As shown in Figs. 3.13A-B, mRNA expression of the pluripotency markers *Oct4* and Nanog decreased considerably in all groups over the course of five days in suspension (**Fig3.9A-B**). Germ layer marker expression on the other hand was highly variable in all three treatment groups. Consequently there were no statistically significant differences among any of the treatment groups in terms of Brachyury (**Fig3.9C**), NeuroD1 (**Fig3.9D**) or Sox17 (**Fig3.9E**) expression. Overall differentiation was biased in favor of ectoderm. BIO treatment especially appeared to encourage ectoderm differentiation. Interestingly, three germ layer differentiation is somewhat attenuated by bFGF, although the morphology and SF-EB survival rate is improved by its inclusion in the EB culture medium.

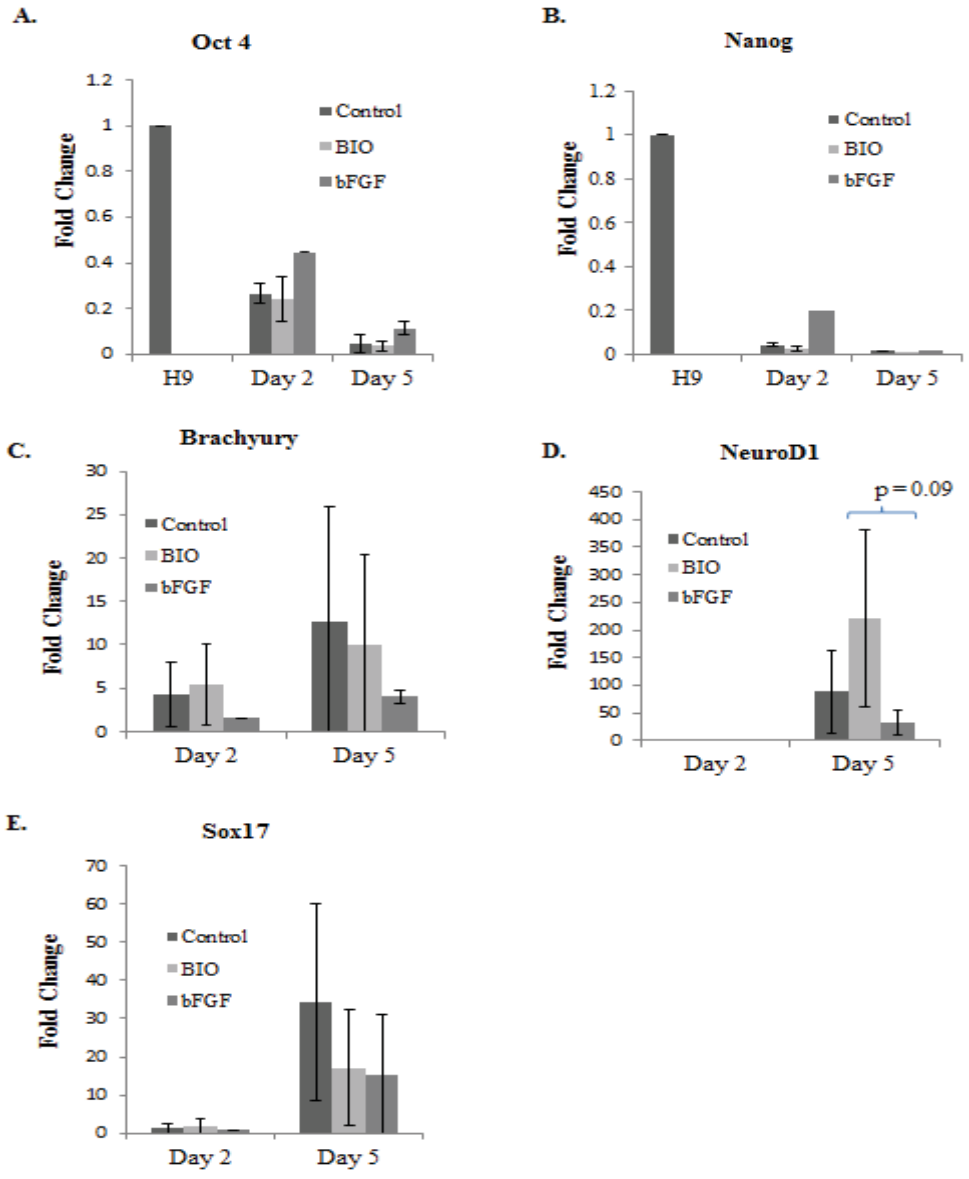

Figure 3.9. qRT-PCR analysis of pluripotency and germ layer markers in differentiating SF-EBs at two time points, day 2 and day 5. Control SF-EBs were grown in suspension in SF-EB medium. BIO and bFGF SF-EBs were grown in suspension in SF-EB medium plus 300 nM BIO or 10 ng/ml bFGF respectively. (A.) Oct 4. (B.) Nanog. (C.) Brachyruy (D.) Neurod1 (E.) Sox 17. Fold changes are determined relative to undifferentiated H9s. β-actin was used as a housekeeping gene. p value was determined by two tailed student's t-test. Error bars indicate standard deviation.

Chapter 4 – Discussion and Future Directions

In this study, we developed a serum free medium for the generation and culture of EBs from mTeSR1 adapted hPSCs and to facilitate the study of signaling pathways that are important for EB growth, cell-cell signaling and differentiation. We found that EBs form readily when cultured in suspension in mTeSR1 compatible SF-EB media, and these SF-EBs maintain their characteristically round morphology for the first 48 hours of suspension culture. However, at later time points SF-EBs begin to degrade, exhibiting defects in morphology and persistently high E-cadherin expression even as pluripotency markers like *Oct 4* and *Nanog* are down regulated.

Supplementing the SF-EB medium with bFGF rescues the morphology of the SF-EBs, and this is in agreement with results obtained by other groups working with mTeSR1 adapted hPSCs. This sensitivity to growth factor withdrawal in EB culture distinguishes mTeSR1 adapted hPSCs from feeder dependent hPSCs, which are routinely grown in suspension in serum free medium without growth factor supplementation [68, 116]. It may be important to consider this sensitivity to growth factor withdrawal when developing EB differentiation protocols for mTeSR1 adapted hPSCs.

In addition to bFGF, we found that modulating the activity of a single kinase, GSK3β, also supports the improved growth, proliferation and morphology of SF-EBs. This suggests a role for GSK3β in the early differentiation events of hPSCs and demonstrates the utility of small molecule inhibitors in dissecting the mechanisms affecting hPSC differentiation and development *in vitro*.

GSK3β participates in numerous signaling pathways and interacts with many substrates that are important for cell proliferation, survival and differentiation. In future studies, it will be important to investigate the signaling pathways that are affected by GSK3β inhibition in SF-EBs. One likely candidate for investigation is the canonical *Wnt* pathway. GSK3β inhibitors are often used as activators of canonical *Wnt* signaling. The timing of the control SF-EBs' degradation in our experiments coincides with the onset of canonical *Wnt* signaling reported for differentiating mEBs [136]. The observed defects in E-cadherin regulation and SF-EB growth during the 5 day experiment is reminiscent of β-catenin null mEBs generated by Lyashenko *et al*. [113]. However our immunostaining results for β-catenin expression in day 5 SF-EBs were equivocal. In future studies, it will be important to target β-catenin more selectively.

Western blots of cytoplasmic and nuclear fractions at multiple time points can determine localization of β-catenin, and luciferase reporter assays can allow for the measurement of β-catenin/TCF complex transcriptional activity [105].

It is quite possible that other signaling pathways besides the canonical *Wnt* pathway are activated in BIO treated SF-EBs. GSK3β inhibitors like BIO act on all of the GSK3β present within the cell [137]. They are highly selective for the protein but cannot distinguish between separate pools of GSK3β. This can be problematic since GSK3β is often regulated by intracellular localization and the formation of complexes with other proteins [85]. These separate pools of GSK3β act on different substrates and participate in different pathways. For example, less than 10% of the GSK3β in a cell is involved in canonical *Wnt* signaling [137]. Thus GSK3β inhibition and canonical *Wnt* signaling are not necessarily synonymous.

Also it is likely that GSK3β was only partially inhibited in the BIO treated SF-EBs as shown in this study, as the concentration of BIO (300 nM) that we used was fairly low compared to the concentrations used by other researchers to activate canonical *Wnt* signaling in monolayer cultures (1-5 μM) [104, 110]. This is notable because other groups have reported that different amounts of GSK3β inhibition in undifferentiated hPSCs exhibit threshold effects, with low concentrations of BIO stabilizing c-myc and high concentrations activating canonical *Wnt* signaling [106]. In our study, a low concentration of BIO was necessary as higher concentrations led to SF-EB agglomeration. In the future, it may be possible to prevent SF-EB agglomeration by culturing the SF-EBs in an orbital shaker or stirred tank bioreactor. This would allow for the use of higher concentrations of GSK3β inhibitors.

It is possible that maintenance of SF- EB morphology only requires the inactivation of a particular pool of GSK3β. Western blots of cytoplasmic and nuclear fractions of SF-EBs can determine the localization of GSK3β as well as its phosphorylation status. High GSK3β activity in the nucleus is associated with cell apoptosis and cell cycle arrest [98]. Potential GSK3β targets that could affect the survival and cell cycle progression of cells within SF-EBs include c-myc, cyclinD1, p53 and p27 [98]. Also in future experiments, flow cytometric analysis and BrdU incorporation assays may be used to assess cell cycle progression and proliferation within SF-EBs.

The effects of GSK3β inhibition on E-cadherin expression suggests that GSK3β inactivation may promote EMTs in SF-EBs. It is not clear whether GSK3β inhibition initiates EMT like events or if GSK3β inhibition permits the survivaland proliferation of cells already undergoing EMT. Our qRT-PCR analysis of the EMT promoting transcription factors Snail, Slug and Twist1 revealed no significant difference between SF-EBs with and without bFGF or BIO treatment. However GSK3β is known to affect the stability of these proteins. Thus western blots may reveal differences in expression between different treatment groups not evident at the level of transcription.

The ability of small molecule inhibitors of GSK3β to support SF-EB survival may prove useful for the development of EB-based hPSC differentiation protocols for the generation of GMP grade somatic cells for applications in regenerative medicine. GSK3β inhibition has been used in concert with other small molecule inhibitors and growth factors to generate definitive endoderm, mesoderm, as well as neural progenitors, neural stem cells and neural crest stem cells [106, 112, 138-140]. Reducing the need for growth factor stimulation has the potential to greatly reduce the cost associated with pluripotent stem cell research. Also selective small molecule inhibitors allow researchers to target specific proteins, and this could deepen our understanding of the signaling pathways controlling early embryological development.

The SF-EB medium may be especially useful in generation of neural progenitors or neural crest cells with small molecules, as the early neural marker NeuroD1 was highly up regulated in of BIO treated SF-EBs (**Fig. 3.12E**). Adopting differentiation protocols that replace growth factors with small molecules promises to reduce costs and allow for the production of matured cell types in more defined conditions [139]. Of course, patterns of three germ layer expression on day 5 were highly variable in all groups, but regardless of treatment, differentiation at 5 days post SF-EB formation was strongly biased towards ectoderm. This result is in agreement with Bock *et al* [141]. In future studies it will be important to examine SF-EB derived cells at later time points to confirm that early differentiation marker expression accurately reflects the ultimate fate decisions of those cells and to characterize these cells' ability to give rise to terminally differentiated cell types.

It is possible that the weak mesendodermal marker expression we observed in all three treatment groups could be due in part to the composition of the SF-EB medium. mTeSR1 has a very high insulin

concentration-- approximately 20 µg/mL-- and since the SF-EB medium is modeled on mTeSR1, it has a similarly high insulin concentration. Freund *et al.* have reported that insulin treatment in hESCs prevents mesendoderm differentiation and favors neuroectodermal differentiation [142] . However another group argues that insulin does not prevent all mesendoderm differentiation, but it does attenuate differentiation into cardiac mesoderm [143]. It might be advantageous in future experiments to find ways of reducing the insulin concentration in the SF-EB medium without compromising the SF-EB medium's compatibility with mTeSR1, especially if the goal is to direct hPSC differentiation into mesendodermal lineages.

In conclusion, we demonstrate that chemical inhibition of GSK3β is sufficient to support the growth of EBs derived from mTeSR1 adapted hPSCs. The use of small molecules to direct hPSC differenitation may help facilitate the development of defined culture conditions, which is necessary step in the transition of hPSCs from bench to clinic.

References

1. Thomson, J.A. et al. Embryonic stem cell lines derived from human blastocysts. *Science* **282**, 1145-1147 (1998).

2. Reubinoff, B.E., Pera, M.F., Fong, C.Y., Trounson, A. & Bongso, A. Embryonic stem cell lines from human blastocysts: somatic differentiation in vitro. *Nat. Biotechnol.* **18**, 399-404 (2000).

3. Takahashi, K. et al. Induction of pluripotent stem cells from adult human fibroblasts by defined factors. *Cell* **131**, 861-872 (2007).

4. Yu, J. et al. Induced pluripotent stem cell lines derived from human somatic cells. *Science* **318**, 1917-1920 (2007).

5. Carey, B.W. et al. Reprogramming of murine and human somatic cells using a single polycistronic vector. *Proc Natl Acad Sci U S A* **106**, 157-162 (2009).

6. Zhou, W. & Freed, C.R. Adenoviral gene delivery can reprogram human fibroblasts to induced pluripotent stem cells. *Stem Cells* **27**, 2667-2674 (2009).

7. Yu, J. et al. Human induced pluripotent stem cells free of vector and transgene sequences. *Science* **324**, 797-801 (2009).

8. Woltjen, K. et al. piggyBac transposition reprograms fibroblasts to induced pluripotent stem cells. *Nature* **458**, 766-770 (2009).

9. Warren, L. et al. Highly efficient reprogramming to pluripotency and directed differentiation of human cells with synthetic modified mRNA. *Cell Stem Cell* **7**, 618-630 (2010).

10. Izpisua Belmonte, J.C., Ellis, J., Hochedlinger, K. & Yamanaka, S. Induced pluripotent stem cells and reprogramming: seeing the science through the hype. *Nat Rev Genet* **10**, 878-883 (2009).

11. Boyd, A.S., Rodrigues, N.P., Lui, K.O., Fu, X. & Xu, Y. Concise review: Immune recognition of induced pluripotent stem cells. *Stem Cells* **30**, 797-803 (2012).

12. Srivastava, A.S., Malhotra, R., Sharp, J. & Berggren, T. Potentials of ES Cell Therapy in Neurodegenerative Diseases. *Curr. Pharm. Design* **14**, 3873-3879 (2008).

13. Lukovic, D., Manzano, V.M., Stojkovic, M., Bhattacharya, S.S. & Erceg, S. Concise Review: Human Pluripotent Stem Cells in the Treatment of Spinal Cord Injury. *Stem Cells* **30**, 1787-1792 (2012).

14. Noguchi, H. Production of pancreatic beta-cells from stem cells. *Current diabetes reviews* **6**, 184-190 (2010).

15. Ameen, C. et al. Human embryonic stem cells: Current technologies and emerging industrial applications. *Crit. Rev. Oncol./Hematol.* **65**, 54-80 (2008).

16. Frantz, S. Embryonic stem cell pioneer Geron exits field, cuts losses. *Nat. Biotechnol.* **30**, 12-13 (2012).

17. Schwartz, S.D. et al. Embryonic stem cell trials for macular degeneration: a preliminary report. *Lancet* **379**, 713-720 (2012).

18. Pouton, C.W. & Haynes, J.M. Pharmaceutical applications of embryonic stem cells. *Adv. Drug Deliv. Rev.* **57**, 1918-1934 (2005).

19. Dvash, T. & Benvenisty, N. Human embryonic stem cells as a model for early human development. *Best Pract. Res. Clin. Obstet. Gynaecol.* **18**, 929-940 (2004).

20. Briggs, J.A. et al. Integration-free induced pluripotent stem cells model genetic and neural developmental features of down syndrome etiology. *Stem Cells* **31**, 467-478 (2013).

21. Yung, S.K. et al. Brief report: human pluripotent stem cell models of fanconi anemia deficiency reveal an important role for fanconi anemia proteins in cellular reprogramming and survival of hematopoietic progenitors. *Stem Cells* **31**, 1022-1029 (2013).

22. Park, I.H. et al. Disease-specific induced pluripotent stem cells. *Cell* **134**, 877-886 (2008).

23. Brennand, K.J. et al. Modelling schizophrenia using human induced pluripotent stem cells. *Nature* **473**, 221-225 (2011).

24. Pera, M.F. & Trounson, A.O. Human embryonic stem cells: prospects for development. *Development* **131**, 5515-5525 (2004).

25. Zhang, X. et al. Derivation of human embryonic stem cells from developing and arrested embryos. *Stem Cells* **24**, 2669-2676 (2006).

26. Boyer, L.A. et al. Core transcriptional regulatory circuitry in human embryonic stem cells. *Cell* **122**, 947-956 (2005).

27. Vallier, L., Alexander, M. & Pedersen, R.A. Activin/Nodal and FGF pathways cooperate to maintain pluripotency of human embryonic stem cells. *J. Cell Sci.* **118**, 4495-4509 (2005).

28. Ludwig, T.E. et al. Derivation of human embryonic stem cells in defined conditions. *Nat. Biotechnol.* **24**, 185-187 (2006).

29. Wang, L. et al. Self-renewal of human embryonic stem cells requires insuhn-like growth factor-1 receptor and ERBB2 receptor signaling. *Blood* **110**, 4111-4119 (2007).

30. Dalton, S. Signaling networks in human pluripotent stem cells. *Curr Opin Cell Biol* (2012).

31. Tesar, P.J. et al. New cell lines from mouse epiblast share defining features with human embryonic stem cells. *Nature* **448**, 196-U110 (2007).

32. Richards, M. et al. Comparative evaluation of various human feeders for prolonged undifferentiated growth of human embryonic stem cells. *Stem Cells* **21**, 546-556 (2003).

33. Prowse, A.B.J., McQuade, L.R., Bryant, K.J., Marcal, H. & Gray, P.P. Identification of potential pluripotency determinants for human embryonic stem cells following proteomic analysis of human and mouse fibroblast conditioned media. *J. Proteome Res.* **6**, 3796-3807 (2007).

34. Greber, B., Lehrach, H. & Adjaye, J. Fibroblast growth factor 2 modulates transforming growth factor beta signaling in mouse embryonic fibroblasts and human ESCs (hESCs) to support hESC self-renewal. *Stem Cells* **25**, 455-464 (2007).

35. Xu, C.H. et al. Feeder-free growth of undifferentiated human embryonic stem cells. *Nat. Biotechnol.* **19**, 971-974 (2001).

36. Kleinman, H.K. & Martin, G.R. Matrigel: Basement membrane matrix with biological activity. *Semin. Cancer Biol.* **15**, 378-386 (2005).

37. Villa-Diaz, L.G., Ross, A.M., Lahann, J. & Krebsbach, P.H. Concise review: The evolution of human pluripotent stem cell culture: from feeder cells to synthetic coatings. *Stem Cells* **31**, 1-7 (2013).

38. Martin, M.J., Muotri, A., Gage, F. & Varki, A. Human embryonic stem cells express an immunogenic nonhuman sialic acid. *Nat. Med.* **11**, 228-232 (2005).

39. Ludwig, T.E. et al. Feeder-independent culture of human embryonic stem cells. *Nat. Methods* **3**, 637-646 (2006).

40. Xu, R.H. et al. Basic FGF and suppression of BMP signaling sustain undifferentiated proliferation of human ES cells. *Nat. Methods* **2**, 185-190 (2005).

41. Sato, N., Meijer, L., Skaltsounis, L., Greengard, P. & Brivanlou, A.H. Maintenance of pluripotency in human and mouse embryonic stem cells through activation of Wnt signaling by a pharmacological GSK-3-specific inhibitor. *Nat. Med.* **10**, 55-63 (2004).

42. Sperger, J.M. et al. Gene expression patterns in human embryonic stem cells and human pluripotent germ cell tumors. *Proc Natl Acad Sci U S A* **100**, 13350-13355 (2003).

43. Braam, S.R. et al. Recombinant vitronectin is a functionally defined substrate that supports human embryonic stem cell self-renewal via alpha V beta 5 integrin. *Stem Cells* **26**, 2257-2265 (2008).

44. Villa-Diaz, L.G. et al. Synthetic polymer coatings for long-term growth of human embryonic stem cells. *Nat. Biotechnol.* **28**, 581-583 (2010).

45. Melkoumian, Z. et al. Synthetic peptide-acrylate surfaces for long-term self-renewal and cardiomyocyte differentiation of human embryonic stem cells. *Nat. Biotechnol.* **28**, 606-U695 (2010).

46. Chen, G.K. et al. Chemically defined conditions for human iPSC derivation and culture. *Nat. Methods* **8**, 424-U476 (2011).

47. Akopian, V. et al. Comparison of defined culture systems for feeder cell free propagation of human embryonic stem cells. *In Vitro Cell. Dev. Biol.-Anim.* **46**, 247-258 (2010).

48. Yoon, T.M. et al. Human Embryonic Stem Cells (hESCs) Cultured Under Distinctive Feeder-Free Culture Conditions Display Global Gene Expression Patterns Similar to hESCs from Feeder-Dependent Culture Conditions. *Stem Cell Rev. Rep.* **6**, 425-437 (2010).

49. Hannoun, Z. et al. The comparison between conditioned media and serum-free media in human embryonic stem cell culture and differentiation. *Cell Reprogram* **12**, 133-140 (2010).

50. Cao, J. et al. Fourier transform infrared microspectroscopy reveals unique phenotypes for human embryonic and induced pluripotent stem cell lines and their progeny. *J Biophotonics* **25**, 201200217 (2013).

51. Tompkins, J.D. et al. Epigenetic stability, adaptability, and reversibility in human embryonic stem cells. *Proc. Natl. Acad. Sci. U. S. A.* **109**, 12544-12549 (2012).

52. Blauwkamp, T.A., Nigam, S., Ardehali, R., Weissman, I.L. & Nusse, R. Endogenous Wnt signalling in human embryonic stem cells generates an equilibrium of distinct lineage-specified progenitors. *Nat Commun* **3** (2012).

53. Ojala, M. et al. Culture Conditions Affect Cardiac Differentiation Potential of Human Pluripotent Stem Cells. *PLoS One* **7** (2012).

54. Sharon, N., Mor, I., Golan-lev, T., Fainsod, A. & Benvenisty, N. Molecular and Functional Characterizations of Gastrula Organizer Cells Derived from Human Embryonic Stem Cells. *Stem Cells* **29**, 600-608 (2011).

55. Fuchs, C. et al. Self-Organization Phenomena in Embryonic Stem Cell-Derived Embryoid Bodies: Axis Formation and Breaking of Symmetry during Cardiomyogenesis. *Cells Tissues Organs* **195**, 377-391 (2012).

56. Ungrin, M.D., Joshi, C., Nica, A., Bauwens, C. & Zandstra, P.W. Reproducible, Ultra High-Throughput Formation of Multicellular Organization from Single Cell Suspension-Derived Human Embryonic Stem Cell Aggregates. *PLoS One* **3** (2008).

57. Maurer, J. et al. Contrasting Expression of Keratins in Mouse and Human Embryonic Stem Cells. *PLoS One* **3** (2008).

58. Li, X.F. et al. Fibroblast growth factor signaling and basement membrane assembly are connected during epithelial morphogenesis of the embryoid body. *J. Cell Biol.* **153**, 811-822 (2001).

59. Sachlos, E. & Auguste, D.T. Embryoid body morphology influences diffusive transport of inductive biochemicals: A strategy for stem cell differentiation. *Biomaterials* **29**, 4471-4480 (2008).

60. Bratt-Leal, A.M., Carpenedo, R.L. & McDevitt, T.C. Engineering the Embryoid Body Microenvironment to Direct Embryonic Stem Cell Differentiation. *Biotechnol. Prog.* **25**, 43-51 (2009).

61. Van Winkle, A.P., Gates, I.D. & Kallos, M.S. Mass Transfer Limitations in Embryoid Bodies during Human Embryonic Stem Cell Differentiation. *Cells Tissues Organs* **196**, 34-47 (2012).

62. Schulz, T.C. et al. A Scalable System for Production of Functional Pancreatic Progenitors from Human Embryonic Stem Cells. *PLoS One* **7** (2012).

63. Carpenedo, R.L. et al. Homogeneous and organized differentiation within embryoid bodies induced by microsphere-mediated delivery of small molecules. *Biomaterials* **30**, 2507-2515 (2009).

64. Ng, E.S., Davis, R.P., Azzola, L., Stanley, E.G. & Elefanty, A.G. Forced aggregation of defined numbers of human embryonic stem cells into embryoid bodies fosters robust, reproducible hematopoietic differentiation. *Blood* **106**, 1601-1603 (2005).

65. Chadwick, K. et al. Cytokines and BMP-4 promote hematopoietic differentiation of human embryonic stem cells. *Blood* **102**, 906-915 (2003).

66. Kehat, I. et al. Human embryonic stem cells can differentiate into myocytes with structural and functional properties of cardiomyocytes. *J. Clin. Invest.* **108**, 407-414 (2001).

67. Khoo, M.L.M. et al. Growth and differentiation of embryoid bodies derived from human embryonic stem cells: Effect of glucose and basic fibroblast growth factor. *Biol. Reprod.* **73**, 1147-1156 (2005).

68. Itskovitz-Eldor, J. et al. Differentiation of human embryonic stem cells into embryoid bodies comprising the three embryonic germ layers. *Mol. Med.* **6**, 88-95 (2000).

69. Mummery, C.L. et al. Differentiation of human embryonic stem cells and induced pluripotent stem cells to cardiomyocytes: a methods overview. *Circ Res* **111**, 344-358 (2012).

70. Antonchuk, J., et al. 7th annual meeting of the International Society for Stem Cell Research; (2009).

71. Antonchuk, J. in Methods in molecular biology (Clifton, N.J.), Vol. 946 523-533 (2013).

72. Shevde, N.K. & Mael, A.A. in Methods in molecular biology (Clifton, N.J.), Vol. 946 535-546 (2012).

73. Dailey, L., Ambrosetti, D., Mansukhani, A. & Basilico, C. Mechanisms underlying differential responses to FGF signaling. *Cytokine Growth Factor Rev.* **16**, 233-247 (2005).

74. Wang, X.F., Lin, G., Martins-Taylor, K., Zeng, H. & Xu, R.H. Inhibition of Caspase-mediated Anoikis Is Critical for Basic Fibroblast Growth Factor-sustained Culture of Human Pluripotent Stem Cells. *J. Biol. Chem.* **284**, 34054-34064 (2009).

75. Zhang, S.C., Wernig, M., Duncan, I.D., Brustle, O. & Thomson, J.A. In vitro differentiation of transplantable neural precursors from human embryonic stem cells. *Nat. Biotechnol.* **19**, 1129-1133 (2001).

76. Li, X.J. et al. Specification of motoneurons from human embryonic stem cells. *Nat. Biotechnol.* **23**, 215-221 (2005).

77. Itsykson, P. et al. Derivation of neural precursors from human embryonic stem cells in the presence of noggin. *Mol. Cell. Neurosci.* **30**, 24-36 (2005).

78. Greber, B. et al. FGF signalling inhibits neural induction in human embryonic stem cells. *Embo J.* **30**, 4874-4884 (2011).

79. Yu, P.Z., Pan, G.J., Yu, J.Y. & Thomson, J.A. FGF2 Sustains NANOG and Switches the Outcome of BMP4-Induced Human Embryonic Stem Cell Differentiation. *Cell Stem Cell* **8**, 326-334 (2011).

80. Israsena, N., Hu, M., Fu, W.M., Kan, L.X. & Kessler, J.A. The presence of FGF2 signaling determines whether beta-catenin exerts effects on proliferation or neuronal differentiation of neural stem cells. *Dev. Biol.* **268**, 220-231 (2004).

81. Ciruna, B. & Rossant, J. FGF signaling regulates mesoderm cell fate specification and morphogenetic movement at the primitive streak. *Dev. Cell* **1**, 37-49 (2001).

82. Ding, V.M.Y. et al. FGF-2 Modulates Wnt Signaling in Undifferentiated hESC and iPS Cells Through Activated PI3-K/GSK3 beta Signaling. *J. Cell. Physiol.* **225**, 417-428 (2010).

83. Hay, E.D. The mesenchymal cell, its role in the embryo, and the remarkable signaling mechanisms that create it. *Dev Dyn* **233**, 706-720 (2005).

84. Moon, R.T., Bowerman, B., Boutros, M. & Perrimon, N. The promise and perils of Wnt signaling through beta-catenin. *Science* **296**, 1644-1646 (2002).

85. Kaidanovich-Beilin, O. & Woodgett, J.R. GSK-3: Functional Insights from Cell Biology and Animal Models. *Frontiers in molecular neuroscience* **4**, 40 (2011).

86. Aberle, H., Bauer, A., Stappert, J., Kispert, A. & Kemler, R. beta-catenin is a target for the ubiquitin-proteasome pathway. *Embo J.* **16**, 3797-3804 (1997).

87. Woodgett, J.R. MOLECULAR-CLONING AND EXPRESSION OF GLYCOGEN-SYNTHASE KINASE-3 FACTOR-A. *Embo J.* **9**, 2431-2438 (1990).

88. Woodgett, J.R. REGULATION AND FUNCTIONS OF THE GLYCOGEN-SYNTHASE KINASE-3 SUBFAMILY. *Semin. Cancer Biol.* **5**, 269-275 (1994).

89. Cross, D.A.E., Alessi, D.R., Cohen, P., Andjelkovich, M. & Hemmings, B.A. INHIBITION OF GLYCOGEN-SYNTHASE KINASE-3 BY INSULIN-MEDIATED BY PROTEIN-KINASE-B. *Nature* **378**, 785-789 (1995).

90. Sutherland, C., Leighton, I.A. & Cohen, P. INACTIVATION OF GLYCOGEN-SYNTHASE KINASE-3-BETA BY PHOSPHORYLATION - NEW KINASE CONNECTIONS IN INSULIN AND GROWTH-FACTOR SIGNALING. *Biochem. J.* **296**, 15-19 (1993).

91. Delcommenne, M. et al. Phosphoinositide-3-OH kinase-dependent regulation of glycogen synthase kinase 3 and protein kinase B/AKT by the integrin-linked kinase. *Proc. Natl. Acad. Sci. U. S. A.* **95**, 11211-11216 (1998).

92. Stambolic, V. & Woodgett, J.R. MITOGEN INACTIVATION OF GLYCOGEN-SYNTHASE KINASE-3-BETA IN INTACT-CELLS VIA SERINE-9 PHOSPHORYLATION. *Biochem. J.* **303**, 701-704 (1994).

93. Fang, X.J. et al. Phosphorylation and inactivation of glycogen synthase kinase 3 by protein kinase A. *Proc. Natl. Acad. Sci. U. S. A.* **97**, 11960-11965 (2000).

94. Saito, Y., Vandenheede, J.R. & Cohen, P. THE MECHANISM BY WHICH EPIDERMAL GROWTH-FACTOR INHIBITS GLYCOGEN-SYNTHASE KINASE 3 IN A431 CELLS. *Biochem. J.* **303**, 27-31 (1994).

95. Ding, Q.Q. et al. Erk associates with and primes GSK-3 beta for its inactivation resulting in upregulation of beta-catenin. *Mol. Cell* **19**, 159-170 (2005).

96. Thornton, T.M. et al. Phosphorylation by p38 MAPK as an alternative pathway for GSK3 beta inactivation. *Science* **320**, 667-670 (2008).

97. Kim, L., Liu, J.C. & Kimmel, A.R. The novel tyrosine kinase ZAK1 activates GSK3 to direct cell fate specification. *Cell* **99**, 399-408 (1999).

98. Sutherland, C. What Are the bona fide GSK3 Substrates? *Int J Alzheimers Dis* **505607**, 18 (2011).

99. Grimes, C.A. & Jope, R.S. The multifaceted roles of glycogen synthase kinase 3 beta in cellular signaling. *Prog. Neurobiol.* **65**, 391-426 (2001).

100. Watcharasit, P. et al. Glycogen synthase kinase-3 beta (GSK3 beta) binds to and promotes the actions of p53. *J. Biol. Chem.* **278**, 48872-48879 (2003).

101. Surjit, M. & Lal, S.K. Glycogen synthase kinase-3 phosphorylates and regulates the stability of p27kip1 protein. *Cell Cycle* **6**, 580-588 (2007).

102. Forde, J.E. & Dale, T.C. Glycogen synthase kinase 3: a key regulator of cellular fate. *Cell Mol Life Sci* **64**, 1930-1944 (2007).

103. Zoumaro-Djayoon, A.D. et al. Investigating the role of FGF-2 in stem cell maintenance by global phosphoproteomics profiling. *Proteomics* **11**, 3962-3971 (2011).

104. Singh, A.M., Bechard, M., Smith, K. & Dalton, S. Reconciling the different roles of Gsk3 beta in "naive" and "primed" pluripotent stem cells. *Cell Cycle* **11**, 2991-2996 (2012).

105. Davidson, K.C. et al. Wnt/β-catenin signaling promotes differentiation, not self-renewal, of human embryonic stem cells and is repressed by Oct4. *Proc Natl Acad Sci U S A* **109**, 4485-4490 (2012).

106. Singh, A.M. et al. Signaling Network Crosstalk in Human Pluripotent Cells: A Smad2/3-Regulated Switch that Controls the Balance between Self-Renewal and Differentiation. *Cell Stem Cell* **10**, 312-326 (2012).

107. Jin, S., Yao, H.T., Krisanarungson, P., Haukas, A. & Ye, K.M. Porous Membrane Substrates Offer Better Niches to Enhance the Wnt Signaling and Promote Human Embryonic Stem Cell Growth and Differentiation. *Tissue Eng. Part A* **18**, 1419-1430 (2012).

108. Carpenter, M.K. et al. Properties of four human embryonic stem cell lines maintained in a feeder-free culture system. *Dev. Dyn.* **229**, 243-258 (2004).

109. Ullmann, U. et al. GSK-3-specific inhibitor-supplemented hESC medium prevents the epithelial-mesenchymal transition process and the up-regulation of matrix metalloproteinases in hESCs cultured in feeder-free conditions. *Mol. Hum. Reprod.* **14**, 169-179 (2008).

110. Sumi, T., Tsuneyoshi, N., Nakatsuji, N. & Suemori, H. Defining early lineage specification of human embryonic stem cells by the orchestrated balance of canonical Wnt/beta-catenin, Activin/Nodal and BMP signaling. *Development* **135**, 2969-2979 (2008).

111. Arnold, S.J. et al. Brachyury is a target gene of the Wnt/beta-catenin signaling pathway. *Mech. Dev.* **91**, 249-258 (2000).

112. Menendez, L., Yatskievych, T.A., Antin, P.B. & Dalton, S. Wnt signaling and a Smad pathway blockade direct the differentiation of human pluripotent stem cells to multipotent neural crest cells. *Proc. Natl. Acad. Sci. U. S. A.* **108**, 19240-19245 (2011).

113. Lyashenko, N. et al. Differential requirement for the dual functions of beta-catenin in embryonic stem cell self-renewal and germ layer formation. *Nat. Cell Biol.* **13**, 753-U365 (2011).

114. Eastham, A.M. et al. Epithelial-mesenchymal transition events during human embryonic stem cell differentiation. *Cancer Res.* **67**, 11254-11262 (2007).

115. Campbell, S., Swann, H.R., Seif, M.W., Kimber, S.J. & Aplin, J.D. CELL-ADHESION MOLECULES ON THE OOCYTE AND PREIMPLANTATION HUMAN EMBRYO. *Hum. Reprod.* **10**, 1571-1578 (1995).

116. Dang, S.M., Gerecht-Nir, S., Chen, J., Itskovitz-Eldor, J. & Zandstra, P.W. Controlled, scalable embryonic stem cell differentiation culture. *Stem Cells* **22**, 275-282 (2004).

117. Watanabe, K. et al. A ROCK inhibitor permits survival of dissociated human embryonic stem cells. *Nat. Biotechnol.* **25**, 681-686 (2007).

118. Ohgushi, M. et al. Molecular Pathway and Cell State Responsible for Dissociation-Induced Apoptosis in Human Pluripotent Stem Cells. *Cell Stem Cell* **7**, 225-239 (2010).

119. Hwang, Y.S. et al. Microwell-mediated control of embryoid body size regulates embryonic stem cell fate via differential expression of WNT5a and WNT11. *Proc Natl Acad Sci U S A* **106**, 16978-16983 (2009).

120. Cai, J.L. et al. Development of antibodies to human embryonic stem cell antigens. *BMC Dev. Biol.* **5**, 7 (2005).

121. Wheelock, M.J. & Johnson, K.R. Cadherins as modulators of cellular phenotype. *Annu Rev Cell Dev Biol* **19**, 207-235 (2003).

122. McCrea, P.D., Gu, D. & Balda, M.S. Junctional music that the nucleus hears: cell-cell contact signaling and the modulation of gene activity. *Cold Spring Harb Perspect Biol* **1** (2009).

123. Heuberger, J. & Birchmeier, W. Interplay of Cadherin-Mediated Cell Adhesion and Canonical Wnt Signaling. *Cold Spring Harbor Perspect. Biol.* **2** (2010).

124. Lim, J. & Thiery, J.P. Epithelial-mesenchymal transitions: insights from development. *Development* **139**, 3471-3486 (2012).

125. Spencer, H.L. et al. E-cadherin inhibits cell surface localization of the pro-migratory 5T4 oncofetal antigen in mouse embryonic stem cells. *Mol. Biol. Cell* **18**, 2838-2851 (2007).

126. Nandadasa, S., Tao, Q., Menon, N.R., Heasman, J. & Wylie, C. N- and E-cadherins in Xenopus are specifically required in the neural and non-neural ectoderm, respectively, for F-actin assembly and morphogenetic movements. *Development* **136**, 1327-1338 (2009).

127. Elkabetz, Y. et al. Human ES cell-derived neural rosettes reveal a functionally distinct early neural stem cell stage. *Genes Dev.* **22**, 152-165 (2008).

128. D'Amour, K.A. et al. Efficient differentiation of human embryonic stem cells to definitive endoderm. *Nat. Biotechnol.* **23**, 1534-1541 (2005).

129. Pruszak, J., Sonntag, K.C., Aung, M.H., Sanchez-Pernaute, R. & Isacson, O. Markers and methods for cell sorting of human embryonic stem cell-derived neural cell Populations. *Stem Cells* **25**, 2257-2268 (2007).

130. Evseenko, D. et al. Mapping the first stages of mesoderm commitment during differentiation of human embryonic stem cells. *Proc. Natl. Acad. Sci. U. S. A.* **107**, 13742-13747 (2010).

131. Zhou, B.H.P. et al. Dual regulation of Snail by GSK-3 beta-mediated phosphorylation in control of epithelial-mesenchymal transition. *Nat. Cell Biol.* **6**, 931-+ (2004).

132. Bachelder, R.E., Yoon, S.O., Franci, C., de Herreros, A.G. & Mercurio, A.M. Glycogen synthase kinase-3 is an endogenous inhibitor of snail transcription: implications for the epithelial-mesenchymal transition. *J. Cell Biol.* **168**, 29-33 (2005).

133. Lander, R. et al. Interactions between Twist and other core epithelial-mesenchymal transition factors are controlled by GSK3-mediated phosphorylation. *Nature communications* **4**, 1542 (2013).

134. Katoh, M. Cross-talk of WNT and FGF signaling pathways at GSK3 beta to regulate beta-catenin and SNAIL signaling cascades. *Cancer Biol. Ther.* **5**, 1059-1064 (2006).

135. Woods, N.B. et al. Brief Report: Efficient Generation of Hematopoietic Precursors and Progenitors from Human Pluripotent Stem Cell Lines. *Stem Cells* **29**, 1158-1164.

136. ten Berge, D. et al. Wnt Signaling Mediates Self-Organization and Axis Formation in Embryoid Bodies. *Cell Stem Cell* **3**, 508-518 (2008).

137. Voskas, D., Ling, L.S. & Woodgett, J.R. Does GSK-3 provide a shortcut for PI3K activation of Wnt signalling? *F1000 biology reports* **2**, 82 (2010).

138. Bone, H.K., Nelson, A.S., Goldring, C.E., Tosh, D. & Welham, M.J. A novel chemically directed route for the generation of definitive endoderm from human embryonic stem cells based on inhibition of GSK-3. *J. Cell Sci.* **124**, 1992-2000.

139. Reinhardt, P. et al. Derivation and Expansion Using Only Small Molecules of Human Neural Progenitors for Neurodegenerative Disease Modeling. *PLoS One* **8**, e59252 (2013).

140. Li, W. et al. Rapid induction and long-term self-renewal of primitive neural precursors from human embryonic stem cells by small molecule inhibitors. *Proc Natl Acad Sci U S A* **108**, 8299-8304 (2011).

141. Bock, C. et al. Reference Maps of Human ES and iPS Cell Variation Enable High-Throughput Characterization of Pluripotent Cell Lines. *Cell* **144**, 439-452.

142. Freund, C. et al. Insulin redirects differentiation from cardiogenic mesoderm and endoderm to neuroectoderm in differentiating human embryonic stem cells. *Stem Cells* **26**, 724-733 (2008).

143. Lian, X.J., Zhang, J.H., Zhu, K.X., Kamp, T.J. & Palecek, S.P. Insulin Inhibits Cardiac Mesoderm, Not Mesendoderm, Formation During Cardiac Differentiation of Human Pluripotent Stem Cells and Modulation of Canonical Wnt Signaling Can Rescue This Inhibition. *Stem Cells* **31**, 447-457 (2013).

Appendix

Preparation of mTeSR1 (Stem Cell Technologies 05850)

1. mTeSR1 basal medium is stored at 4 °C. The 5 x supplement is kept at -20 °C until use.
2. Thaw 100 ml bottle of 5 x supplement.
3. Aliquot 5 x supplement to 10 ml aliquots in 15 ml centrifuge tubes (Corning 430790).
4. Store aliquots at -20 °C.
5. To make 50 ml of mTeSR1:
    a. 40 ml of mTeSR1 basal medium
    b. 10 ml 5 x supplement
6. Mix well.
7. mTeSR1 can be stored at 4 °C for two weeks.

Aliquoting BD Matrigel (BD Biosciences 354230)

1. Matrigel is liquid at 4 °C, but it gels rapidly at room temperature. So aliquot Matrigel under aseptic conditions and keep all reagents on ice.
2. Thaw Matrigel on ice at 4 °C.
3. In biological safety cabinet, make 10 and 30 µl aliquots of Matrigel in 1.5 ml eppendorf tubes (VWR 20170-38).
4. Aliquots are stored at – 80 °C.

Coating tissue culture treated plates with BD Matrigel

1. Thaw aliquot of BD Matrigel at 4 °C.
2. Dilute Matrigel at 1:150 in DMEM/F-12 (Hyclone SH30261.01), e.g. 10 µl in 1.5 ml DMEM/F12
3. Add Matrigel to plate:
    a. 1 ml for 35 mm dish
    b. 2.5 ml for 60 mm dish
    c. 7.5 ml for 100 mm dish
4. Let stand in the hood for at least 1 hour before plating cells.

Thawing hPSCs for culture in mTeSR1

1. Coat a 35 or 60 mm tissue culture treated plate (Corning 430165, 430166) with BD Matrigel
2. Prewarm 7 ml of mTeSR1 to dilute freezing medium plus enough mTeSr1 to resuspend and culture the hPSCs (e.g. 2 ml for a 35 mm dish, 4 ml for 60 mm dish).
3. Retrieve cell aliquot from liquid nitrogen storage.
4. Place aliquot in 37 °C water bath, but be careful to not allow the cap to become submerged, as this may lead to contamination.
5. Gently swirl the aliquot until only a small bit of ice remains.
6. Take the aliquot into a biological safety cabinet.
7. Transfer aliquot to a 15 ml centrifuge tube.
8. Add prewarm mTeSR1 to the tube dropwise to dilute the aliquot in 7 ml prewarmed mTeSR1.
9. Centrifuge the cell suspension for 5 minutes at 300 *x g*.
10. Apsirate the supernatant.
11. Resuspend cell pellet in the appropriate volume of mTeSR1 (2 or 4 ml usually).
12. Apsirate DMEM/F-12/Matrigel solution from the tissue culture treated plate.
13. Transfer the mTeSR1/cell suspension to the plate.
14. Label the plate with cell type, passage number, date and initials.
15. Gently shake the plate back and forth and side to side to evenly distribute the colonies on the plate.
16. Place plate in 5 % CO_2 incubator at 37 °C.
17. Change hPSC medium every day until ready for passage.

Preparing mTeSR1 adapted hPSCs for cryopreservation

1. mTeSR1 adapted cells are cryopreserved in mFreSR medium (Stem Cell Technologies 05854).
2. Culture hPSCs in mTeSR1 until ready for passage.
3. Aspirate culture medium in biological safety cabinet.
4. Incubate hPSCs with prewarmed 1 mg/ml dispase (Stem Cell Technologies 07923) for 7 minutes or until the edges of the colonies begin to curl.
5. Aspirate dispase.

6. Rinse the cells three times with DMEM/F-12.
7. Add enough prewarmed mTeSR1 to cover cells.
8. With 5 ml plastic pipette, expel medium while scraping the plate to remove colonies. Be careful to leave the colonies as big as possible. Do not triturate.
9. Transfer to 15 ml tube.
10. Centrifuge at 300 *x g* for 5 minutes.
11. Aspirate medium.
12. Resuspend in appropriate volume of mFreSR (1 ml per 10^6 cells or 1 ml per 35 mm dish).
13. Transfer cell 1 ml suspension to each cryopreservation vial (Greiner Bio-one Cry-S).
14. Label vial with cell type, passage number, date and initials.
15. Place vial in Nalgene Cryo-1 (5100-0001)filled with isopropyl alcohol (Sigma Aldrich I9030)
16. Place in -80 °C for 24 hours.
17. Place in liquid nitrogen storage.

Passaging mTeSR1 adapted hPSCs

1. The cells receive medium changes every day and are passaged every 3-4 days.
2. Split ratios were 1:4 or 1:5.
3. Coat new dishes with Matrigel using protocol “Coating tissue Culture Treated Plates With Matrigel”.
4. Inspect colonies for signs of differentiation before passaging, and colonies that appear differentiated should be removed by scraping with a plastic pipette tip.
5. Aspirate cell culture medium.
6. Incubate cells in 1 mg/ml dispase (Stem Cell Technologies) for 7 minutes or until the edges of the colonies began to curl.
7. Aspirate dispase and rinse three times in DMEM/F-12
8. Add enough mTESR1 to cover the cells.
9. Use a glass 5 ml pipette to scrape the colonies off the surface of the dish.
10. Transfer cell aggregates to a 15 ml centrifuge tube.

11. The colonies were broken into smaller pieces by pipetting up and down several times with a 5 ml glass pipette.
12. Resuspend in the appropriate volume of medium.
13. Aspirate Matrigel/DMEM/F-12 from new dishes.
14. Transfer cell aggregates to their new Matrigel coated dishes.
15. Inspect the dishes by light microscope to ensure that the aggregates are the right size (~50-60 µm in diameter).
16. Place in a 37 °C incubator with 5% CO_2.
17. Medium should be changed every day.

Knockout serum replacement containing embryoid body medium

Using aseptic technique, combine the following ingredients:

For 50 ml Medium			
DMEM/F-12	39 ml	Hyclone	SH30261.01
Knockout serum replacement	10 ml	Invitrogen	10828-028
β-mercaptoethanol	500 µl	EMD Millipore	ES-007-E
Non-Essential Amino Acids	500 µl	Hyclone	SH30238.01

Mix well and store at 4 °C for up to 2 weeks.

L-Ascorbic acid

1. Dissolve 75 mg of L-ascorbic acid in 25 ml of water. Concentration of stock solution is 3 mg/ml.
2. Sterilize with 0.2 um filter (Corning 431224)
3. Store at -20 C in 1 ml aliquots.

Na Selenite

1. Dissolve 7 mg of Na Selenite in 100 ml of water. Concentration of the stock solution is .07 mg/ml.
2. Sterilize with 0.2 um filter (Corning 431224)
3. Store at -20 C in 1 ml aliquots.

Thiamine HCl

1. Dissolve 50 mg Thiamine HCl acid in 25 ml of water. Concentration of stock solution is 2 mg/ml.
2. Sterilize with 0.2 um filter (Corning 431224)
3. Store at -20 C in 1 ml aliquots.

Bovine Serum Albumin

1. Dissolve 1.45 g BSA in 14.5 ml water. Gently shake to dissolve. Concentration of stock solution is 100 mg/ml.
2. Sterilize with 0.2 um filter (Corning 431224)
3. Use immediately to prepare SF-EB medium.

Glutathione (reduced)

1. Dissolve 50 mg Glutathione in 25 ml of water. Concentration of stock solution is 2 mg/ml.
2. Sterilize with 0.2 um filter (Corning 431224)
3. Store at -20 C in 1 ml aliquots.

Sodium chloride

1. Dissolve 3 g Sodium Chloride in 8.5 ml of water.
2. Bring total volume to 10 ml.
3. Sterilize with 0.2 um filter (Corning 431224)
4. Store at 4° C.

Sodium Bicarbonate

1. Dissolve 900 mg sodium bicarbonate in 10 ml water.
2. Sterilize with 0.2 um filter (Corning 431224)
3. Store at 4° C.

100 ml of mTeSR1 compatible SF-EB medium

1. Thaw frozen stock solutions.
2. Combine ingredients in the following amounts:

Ingredient	Volume (ml)
DMEM F-12	79.34824956
Thiamine HCl	0.3
Glutathione reduced	0.105
Lipids	0.194150441
Trace B	0.2
Trace C	0.1
NEAA	1
Betamercaptoethanol	1
Bovine Serum Albumin	12.96
Insulin Transferrin Selenium solution	2
L-Ascorbic Acid	1.6666
Na selenite	0.022
Sodium Bicarbonate	0.604
NaCl	0.63
L-Glutamine or Glutamax	0.5

Mix thoroughly.

3. If necessary, bring pH to 7.3 and filter.
4. Store at 4 °C.

SF-EB Formation Protocol

1. When hPSC dishes are 70-90% confluent and maintained undifferentiated (cells should not be differentiated at this stage), incubate the cells at 37 °C with 0.5 mg/ml dispase in DMEM/F12 for 30-40 minutes, or until the colonies began to lift off of the plate.
2. Gently shake the plate to dislodge the colonies.
3. Do not aspirate. Tip the dish and dislodge any remaining adherent colonies off with DMEM/F12.
4. Transfer cell colony suspension to a 15 ml centrifuge tube.
5. Allow cell aggregates to sediment by gravity, and gently aspirate the dispase solution.
6. Rinse aggregates three more times in DMEM/F12.
7. Resuspend aggregates in EB medium.
8. Seed aggregates into six well ultra-low attachment plates (Costar 3471)

9. If the EBs are formed from a 100 mm dish, then resuspend in 12 ml SF-EB medium and add 2 ml per well of the 6 well plate.
10. Add 1 additional ml of EB medium to each well to bring the final volume to 3 ml.
11. Place in a 37 °C incubator with 5% CO_2.
12. Medium is refreshed on day 1 post EB formation and then every other day after that.
    a. Tip the plate toward you.
    b. Aspirate 2 ml medium without disturbing EBs.
    c. Add 2 ml of prewarmed EB medium.

RNA Extraction Protocol For hPSC Derived Embryoid Bodies (EBs)

Specialized Materials:

Qiagen RNeasy Mini kit (Cat # 74134)

Proteinase K (20 mg/ml) (Ambion Cat #AM2546)

Omni TH tissue homogenizer.

Qiagen RNase free DNase set (79254)

Protocol:

1. Transfer suspension EBs to a 15 ml tube and allow them to sink to the bottom of the tube by gravity.
2. Gently aspirate the EB medium out of the plates.
3. Rinse the EBs with 1 ml PBS and transfer to a 1.5 ml eppendorf tube.
4. Centrifuge the tube for a few seconds.
5. Gently aspirate the PBS.
6. At this point the EB pellet can be stored in a –80 °C freezer until use.
7. Before beginning RNA extraction, add 10 µl of 2-mercaptoethanol to every 1 ml of RLT buffer you intend to use.
8. Add 300 µl RLT buffer to the EB pellet.
9. Gently vortex the sample to facilitate lysis.
10. Lyse and homogenize the sample using an Omni TH tissue homogenizer.
11. Add 590 µl of RNAse free water to the sample.

12. Add 10 µl of Proteinase K (20 mg/ml solution) and mix.
13. Incubate the mixture in a 55 °C water bath for 10 minutes.
14. Centrifuge at room temperature at 10,000 *x g* for 3 minutes. After centrifugation, there should be a pellet of debris on the bottom of the tube.
15. Transfer the supernatant to a new tube, being careful not to disturb the pellet.
16. Add 450 µl of 100% ethanol to the lysate and mix.
17. Transfer 700 µl of lysate to an RNeasy spin column and centrifuge at 12,000 rpm for 15 seconds. Discard the flow through.
18. Repeat step 17 in the same spin column until all the lysate is used.
19. Add 350 µl of RW1 buffer to the spin column and centrifuge for 15 seconds. Discard the flow through.
20. In separate tube, mix 10µl DNase solution with 70 µl of RDD buffer.
21. Add 80 µl of solution from step 20 to the column.
22. Allow to sit at room temperature for 15 minutes.
23. Add 350 µl of RW1 buffer to the spin column and centrifuge for 15 seconds. Discard the flow through.
24. Add 500 µl of RPE buffer to the spin column and centrifuge for 15 seconds. Discard the flow through.
25. Add 500 µl of RPE buffer to the spin column and centrifuge for 2 minutes. Discard the flow through.
26. Transfer the spin column to a new collection tube and centrifuge for 1 minute in order to dry the column.
27. Transfer the spin column to a new 1.5 ml eppendorf tube. Add 30-50 µl of RNAse free water directly to the column and centrifuge for 1 minute to elute the RNA.
28. Label the tube and store at – 20 C for downstream processes.

Reverse Transcription

1. Reverse transcription was carried out using Applied Biosystems High Capacity cDNA reverse transcription kit (Catalog # 4368814) using manufacturer's protocol.

2. Reaction was set up as follows in 1.5 ml eppendorf tubes:
    a. 2 µl 10x RT Buffer.
    b. 0.8 µl 25x dNTP mix.
    c. 2 µl 10x RT random primers.
    d. 1 µl Multiscribe reverse transcriptase.
    e. 4.2 µl RNase free water.
    f. 2 µg of RNA in Rnase free water to a total reaction volume of 20 µl.
3. Mix well.
4. allow reaction to take place at 25 °C for 10 minutes.
5. 37°C for 2 hours.
6. 85 °C for 5 minutes.
7. The cDNA was stored at - 20 °C.

qRT-PCR Primer design

1. Sequence for gene of interest is copied from the NCBI database.
2. Using MIT's online primer design tool Frodo (http://frodo.wi.mit.edu/):
    a. Paste sequence into user interface.
    b. Product size range set between 100-200 base pairs.
    c. Set concentration of monovalent cations to 60 mM.
    d. Click "Pick Primers".
3. Check candidate primers for specificity in NCBI database:
    a. On gene of interest mRNA page, select "Pick Primers".
    b. Paste candidate primers into appropriate fields.
    c. Click "Get Primers".
    d. Repeat process until a primer with high specificity is found.

Primer reconstitution

1. Primers are briefly centrifuged (a few seconds).
2. Primers are reconstituted to 50 mM based on product sheet of primer.

3. All primers purchased from Eurofins.
4. Primers are further diluted to 6.25 mM in 1.5 ml eppendorf tubes.

qRT-PCR protocol

1. qRT-PCR carried out using the Power SYBR Green PCR Master Mix (Applied Biosystems 4368708).
2. Individual reaction mix consists of:
    a. 12.5 µl SYBR master mix.
    b. 2 µl forward primer stock solution.
    c. 2 µl reverse primer stock solution.
    d. 2.5 µl cDNA template (40 ng or 100 ng reactions)
    e. Water to 25 µl.
3. All components kept on ice when not in use.
4. The reactions were carried out on an Eppendorf realplex4.
5. The temperature ramping speed of the instrument was adjusted to 9600 emulation mode.
    a. Denaturation step set to 13%.
    b. Annealing step set to 30%.
6. The cycle settings were as follows:
    a. 10 minutes 95 ° C Polymerase activation step
    b. 15 seconds 95 ° C Denaturation step.
    c. 30 seconds 60 ° C Annealing step
    d. 30 seconds 72 ° C Extension step
    e. b-d are repeated 40x.
    f. Melting curve.
7. β-actin was selected as housekeeping gene.
8. In most cases, undifferentiated H9 hESCs used as calibrator.
9. Fold change calculations were performed using the ΔΔCt method.
    a. $\Delta Ct_{(sample)} = Ct_{GOI} - Ct_{\beta\text{-actin}}$
    b. $\Delta Ct_{(calibrator)} = Ct_{GOI} - Ct_{\beta\text{-actin}}$

c. $\Delta\Delta Ct = \Delta Ct_{(sample)} - \Delta Ct_{(calibrator)}$

d. Fold change = $2^{-\Delta\Delta Ct}$.

4% Paraformaldehyde

1. Weigh out 1.2 g of paraformaldehyde (Sigma Aldrich P6148)
2. Add 19 ml of water.
3. Heat to 60 °C.
4. Add 5 M NaOH 10 µl at a time until paraformaldehyde completely dissolves.
5. Add 3 ml of 10 x PBS.
6. Bring volume of solution to 30 ml with water.
7. Adjust pH to 7.2 with 5 M HCl.
8. Store at 4 °C for up to 1 week.

Sucrose solution

7.5% solution

1. Weigh out 2.25 g sucrose (Fluka 84097)
2. Dissolve in 30 ml 1x PBS (Cellgro 21-031-CV)
3. Store at 4 °C.

15% solution

1. Weigh out 4.5 g sucrose (Fluka 84097)
2. Dissolve in 30 ml 1x PBS (Cellgro 21-031-CV).
3. Store at 4 °C.

Immunostaining - fixing

1. Transfer suspension EBs to a 15 ml tube and allow them to sink to the bottom of the tube by gravity.
2. Gently aspirate the EB medium.
3. Rinse the EBs with 1 ml PBS and transfer to a 24 well plate.
4. Gently aspirate the PBS.

5. Fix EBs is 4% paraformaldehyde for 20 minutes
6. Aspirate paraformaldehyde without disturbing EBs.
7. Rinse with PBS and aspirate.
8. Incubate EBs with 7.5 % sucrose solution for 3 hours at room temperature.
9. Carefully aspirate solution.
10. Incubate with 15% sucrose solution overnight at 4°C.
11. Carefully transfer EBs to a 15x15x5 mm vinyl freezing medium mold (Tissue Tek).
12. Aspirate sucrose solution.
13. Add enough freezing medium to fill the mold (Triangle Biomedical Sciences TFM-5).
14. Molds are frozen at -20 ºC and then either stored at – 80 ºC or used immediately for cryosectioning.

Immunostaining – Cryosectioning

1. Triangle Biomedical Systems Minotome Plus is set to – 20 °C.
2. If the samples had been stored at – 80 °C, place them in the microtome to allow them to come up to temperature. Sample will be brittle if sections are made just after removing from – 80 °C.
3. To make 8 µm sections, set the index post to 4.
4. Place a small amount of tissue freezing medium on the specimen holder.
5. Mount the sample on the specimen holder, pushing the sample out of the sample mold.
6. Let sit in – 20 °C until sample adheres to the sample holder.
7. Mount the sample to the specimen orientation assembly.
8. Mount a disposable blade (TBS Shur-Sharp) to the knife assembly.
9. Advance the specimen to a point where the surface of the specimen is almost touching the blade.
10. Orient the specimen to the blade such that the blade will cut across the specimen evenly.
11. Take your time here. The EBs tend to settle near the bottom of the sample mold before the tissue freezing medium freezes, and this means that when the sample is mounted to the sample holder, many of the EBs will be sitting near the top of the frozen sample. Most of the really good

sections that you can hope to get will be made in the first few cuts, so it is important to make sure the sample and the blade are properly oriented from the start.

12. Also adjust the anti-roll plate so that it is almost even with the tip of the blade.
13. Start making cuts. If everything is set up correctly, the section should come out underneath the antiroll plate in one thin sheet. If this is not working, sometimes it helps to have the anti-roll plate raised when you begin the cut and then press the anti-roll plate down into position as you are making the cut. The timing of this move is a little tricky at first, but it gets much easier with just a little practice.
14. Transfer the sections to poly-L-lysine coated slides (Electron Microscopy Sciences #63410).
15. Check the slide under a light microscope to make sure you are catching the EBs.
16. Allow slides to sit at room temperature for 30 minutes and then store them at – 80 ° C until ready for staining.

0.5% Saponin

1. Combine 100 mg Saponin (Sigma 47036) with 20 ml water in 50 ml tube.
2. Gently vortex to mix. Keep settings low, because the solution will foam if vortexed too strongly.

Immunostaining – Immunofluorescence

1. Slides were removed from – 80 °C and allowed to air dry for 30 minutes.
2. Incubate samples in 0.5% Saponin in PBS for 10 minutes to permeablize the cells.
3. Rinse slides 3x with PBS.
4. Block samples with 1% BSA (Fisher Scientific BP1600-100) in PBST for 30 minutes.
5. Dilute antibody in 1% BSA in PBST.
6. Incubate sample in antibody for 1 hour at room temperature.
7. Decant solution and wash 3x with PBS, 5 minutes each wash.
8. Dilute secondary antibodies in 1% BSA in PBS.
9. Incubate secondary antibodies for 1 hour in the dark.
10. Decant solution and rinse 3x with PBS in the dark.
11. Stain nuclei with DAPI 1:100 dilution in PBS for 1 minute in the dark.

12. Rinse with PBS.
13. Visualize with Olympus IX71 Fluorescent Microscope and Slide Book software.

RIPA Buffer

1. 150 mM Sodium Chloride (Acros 327300010)
2. 1% TritonX-100 (Acros 327371000)
3. 0.5% sodium deoxycholate (Sigma Aldrich D6750)
4. 0.1% sodium dodecyl sulphate (SDS) (VWR VW1495-04)
5. 50 mM Tris (Cal Biochem 9210)

Tris-Cl/SDS (pH6.8)

1. 40 ml H_2O
2. 1.51 g Tris-Base (Cal Biochem 9210)
3. 0.1 g SDS (VWR VW1495-04)
4. Adjust pH to 6.8.

Loading Buffer

1. 7 ml 4x Tris-Cl/SDS (pH 6.8)
2. 3 ml glycerol (Fisher BP229-1)
3. 1 g SDS (VWR VW1495-04)
4. 0.93 g DTT (Gold Biotechnology DTT10)
5. Bromophenol blue (Sigma Aldrich B0126)

Preparation of PAGE Gel

1. 10% separating gel (0.75mm)
    a. 1.9 ml dH_2O
    b. 1.3 ml 1.5 M Tris (pH 8.8)
    c. 1.7 ml 30% acrylamide (Shelton Scientific IB70022)
    d. 50 µl 10% SDS (VWR VW1495-04)

e. 50 µl 10% APS (Sigma Aldrich A3678)

f. 2 µl TEMED (Amersham Biosciences 17-1312-01)

2. 5% stacking gel

a. 1.4 ml dH_2O

b. 250 µl 1.0 M Tris (pH 6.8)

c. 330 µl 30% acrylamide (Shelton Scientific IB70022)

d. 20 µl 10% SDS (VWR VW1495-04)

e. 20 µl 10% APS (Sigma Aldrich A3678)

f. 2 µl TEMED (Amersham Biosciences 17-1312-01)

SDS Page buffer

1. 100 ml 10x Tris/Glycine/SDS buffer (BIO-RAD 161-0732)
2. 900 ml nanopure water

Transfer Buffer

1. 100 ml 10x Tris/Glycine buffer (BIO-RAD 161-0734)
2. 200 ml methanol (Fisher Scientific BP1105-4)
3. 700 ml nanopure water

Western Blot

1. Transfer suspension EBs to a 15 ml tube and allow them to sink to the bottom of the tube by gravity.
2. Gently aspirate the EB medium.
3. Rinse the EBs with 1 ml PBS and transfer to a 1.5 ml eppendorf tube.
4. Centrifuge the tube for a few seconds.
5. Gently aspirate the PBS.
6. Add 300 µl of cold RIPA lysis buffer with 1 mM PMSF (Pierce 36978) to tube.
7. Homogenize the sample using Omni TH tissue homogenizer.
8. Maintain agitation for 30 minutes at 4 °C.
9. Centrifuge at 4 °C for 15 minutes.

10. Remove supernatant from tube and place in a new eppendorf tube.
11. Combine 1:1 ratio of loading buffer with sample.
12. Heat mixture at 95 °C for 5 minutes.
13. Briefly vortex sample.
14. Load 20 µl sample into each lane of gel along with molecular weight marker Pageruler Plus Prestained Protein Ladder (Thermo Scientific 26619).
15. Run gel on BIO-RAD Power Pac Universal 120 minutes at 90 V.
16. Wet transfer is performed using a nitrocellulose membrane (BIO-RAD 1101093) for 60 minutes at 150 V.
17. Block membrane in 5% milk (BIO RAD 170-6404) for 1 hour at 25 ° C.
18. Anti-Beta Catenin Rabbit monoclonal antibody (Abcam ab32572) is diluted 1:5000 in 5% milk.
19. Anti-Beta actin antibody (Sigma Aldrich A3854) is diluted 1:30000 in 5% milk.
20. Incubate membrane with primary antibody overnight at 4 ° C.
21. Rinse 3x in PBST, 5 minutes per wash.
22. Incubate membrane with secondary antibody goat polyclonal anti rabbit conjugated to HRP (Rockland 611-1302) for 1 hour at room temperature with agitation.
23. Rinse 3x in PBST, 5 minutes per wash.
24. Develop using SuperSignal West Pico Chemiluminescent Substrate (Thermo Scientific 34077).
    a. Mix substrate solutions ina 1:1 ratio
    b. Incubate with membrane for 5 minutes in dark.
    c. Drain excess solution.
    d. Cover blot with clear plastic wrap.
25. Take images with BIO RAD Universal Hood II.